UNIVERSIDADE FEDERAL DO AMAPÁ
PROGRAMA DE PÓS-GRADUAÇÃO EM CIÊNCIAS FARMACÊUTICAS

LENIR CABRAL CORREIA

Triagem virtual baseada em fitocanabinoides para atividade antiobesidade

Macapá
2020

LENIR CABRAL CORREIA

Triagem virtual baseada em fitocanabinoides para atividade antiobesidade

Dissertação apresentada ao Programa de Pós-Graduação em Ciências Farmacêuticas da Universidade Federal do Amapá para obtenção do Título de Mestre em Ciências Farmacêuticas.

Orientadora: Profª Drª Lorane Izabel da Silva Hage Melim

Macapá
2020

Dados Internacionais de Catalogação na Publicação (CIP)
Biblioteca Central da Universidade Federal do Amapá
Elaborada por Cristina Fernandes – CRB-2/1569

Correia, Lenir Cabral.
Triagem virtual baseada em fitocanabinoides para atividade antiobesidade. / Lenir Cabral Correia; Orientadora, Lorane Izabel da Silva Hage Melim. – Macapá, 2020.
55 f.

Dissertação (Mestrado) – Universidade Federal do Amapá, Coordenação do Programa de Pós-Graduação em Ciências Farmacêuticas.

1. Docking molecular. 2. Relação estrutura-atividade. 3. Canabinoides naturais. I. Melim, Lorane Izabel da Silva Hage, orientadora. II. Fundação Universidade Federal do Amapá. III. Título.

616.398 C824t
CDD. 22 ed.

Programa de Pós-Graduação em Ciências Farmacêuticas
da Universidade Federal do Amapá

BANCA EXAMINADORA

Aluno(a): Lenir Cabral Correia

Orientador(a): Profª Drª Lorane Izabel da Silva Hage Melim

Profª Drª Lorane Izabel da Silva Hage Melim / Presidente
Professor Titular do Curso de Farmácia da Universidade Federal do Amapá, UNIFAP.

Prof. Dr. Josivan Da Silva Costa / Membro Titular
Professor Temporário do Curso de Química da Universidade Estadual do Amapá, UEAP.

Prof. Dr. Irlon Maciel Ferreira / Membro Titular
Professor Titular do Curso de Química da Universidade Federal do Amapá, UNIFAP.

Data: 12/03/2020

Dedico este trabalho a Deus, minha orientadora, meus pais, meu esposo e meu pequeno herdeiro Emanuel.

AGRADECIMENTOS

Ao divino criador, que me proporcionou a oportunidade e capacidade de iniciar e concluir mais este projeto;

Aos meus pais por me incentivarem sempre a não parar de buscar o melhor;

Ao meu marido, por me lembrar sempre dos meus objetivos e sonhos de vida;

Aos amigos do PharMedChem, por sempre estarem disponíveis para ajudar e sempre instigando à melhora da qualidade de cada trabalho apresentado;

E à minha orientadora, por sempre estar disponível para sanar desde a menor e mais óbvia dúvida, até o arremate final do artigo.

SUMÁRIO

LISTA DE TABELAS

LISTA DE FIGURAS

SÍMBOLOS, SIGLAS E ABREVIATURAS

ADME	Absorption, Distribution, Metabolism, and Excretion
AEA	Anandamide
ALA	Alanine
AR	Aromatic Region
ARG	Arginine
ASN	Asparagine
ASP	Aspartate
BMI	Body Mass Index
Caco2	Intestinal Cells
CBC	Cannabichromene
CBD	Cannabidiol
CBDN	Cannabinoidiol
CBE	Cannabielsoin
CBG	Cannabigerol
CBL	Cannabicyclol
CBN	Cannabinol
CBT	Cannabitriol
CNS	Central Nervous System
CYS	Cysteine
EC’s	Endogenous cannabiboids
ECL	Extracellular Loop
HA	Hydrogen acceptor
HBA	Hydrogen Bond-Accepting Region
HD	Hydrogen donnor

HIS	Histidine
HOA	Human Oral Absorption
HPO	Hydrophobic Region
ICL	Intracelullar Loop
ILE	Isoleucine
LEU	Leucine
LogBB	Blood-Brain-Permeation
LogKhsa	Human Serum Albumin
MAPK	Mitogen-activated protein kinase
MDCK	Renal Cells
MET	Metionine
MW	Molecular Weight
Pa	Probability of Being Active
PASS	Predicition of Activity Spectra for Substances
PDB	Protein Data Bank
PHE	Phenylalanine
Pi	Probability of Being Inactive
PSA	Polar Surface area
rCB	Receptor Cannabiboid
RMSD	Root Mean Square Deviation
RO5	Rulo of Five
SER	Serine
STARS	Reliability
THC	Tetrahydrocannabinol
THR	Threonine
TM	Transmembrane domains
TRP	Tryptophan

TYR	Tyrosine
WHO	World Health Organization
2-AG	2-arachidonoyl glycerol
Δ9-THC	Delta-9-tetrahydrocnannabinol
Δ8THC	Delta-8-tetrahydrocannabinol

RESUMO

Triagem virtual baseada em fitocanabinoides para atividade antiobesidade

Introdução: A busca por alternativas farmacológicas para combater a obesidade baseia-se no desenvolvimento de compostos que auxiliem na perda de peso, sendo utilizados com segurança e eficácia por um longo período. O sistema endocanabinoide está relacionado à obesidade, aumentando os sinais orexigênicos e reduzindo os sinais de saciedade. A avaliação *in silico* através de triagem virtual e modelagem molecular dos fitocanabinoides de *Cannabis sativa* para este fim decorre do seu potencial polifarmacêutico e da existência de fármacos canabinoides sintéticos que já apresentaram esse resultado. **Objetivo:** Realizar triagem virtual baseada no farmacóforo de fitocanabinoides de *C. sativa*, para buscar agentes antiobesidade com potencial para interagir com o receptor canabinoide 1 (rCB1). **Metodologia:** A triagem virtual incluiu a predição de atividade biológica, a avaliação das propriedades físico-químicas, farmacocinéticas e toxicológicas dos canabinoides (para a obtenção de um farmacóforo de referência) e das moléculas ZINC, bem como o docking molecular no rCB1(PDB:5U09). **Resultados e discussões:** O farmacóforo obtido revelou um modelo de 5 pontos, com uma região aceptora de hidrogênio e quatro regiões hidrofóbicas e este foi submetido ao servidor ZINC para triagem virtual, onde foram obtidas 78 moléculas que sinalizaram atividade antagonista sobre rCB1, além de atividade antiobesidade. Dentre as moléculas ZINC avaliadas, após análise de seus perfis físico-químicos, farmacocinéticos e toxicológicos, as ZINC33053402 e ZINC19084698 apontaram como promissores agentes antiobesidade. **Conclusões:** O melhor perfil das moléculas de ZINC triadas para atuar como antagonista da rCB1 na atividade periférica antiobesidade foram: ZINC33053402 e ZINC19084698 (por apresentar ligação chave para o bloqueio do agonista endocanabinoide da anandamida) e alto GoldScore. Além disso, essas moléculas têm um possível fator favorável à segurança do uso de um antagonista canabinoide em nível periférico, devido ao seu perfil farmacocinético, o que pode superar as barreiras dos efeitos adversos inerentes a essa classe farmacológica.

Palavras-Chave: Docking molecular; Relação estrutura-atividade; Canabinoides naturais; rCB1; Triagem Virtual.

Agradecimentos: Laboratório de Química Farmacêutica e Medicinal (PharMedChem - UNIFAP), Departamento de Ciências Farmacêuticas (Faculdade de Ciências Farmacêuticas de Ribeirão Preto – USP) e Departamento de Química (Faculdade de Filosofia, Ciências e Letras de Ribeirão Preto – USP).

ABSTRACT

Virtual screening based on phytocannabinoids for anti-obesity activity

Introduction: The search for pharmacological alternatives to combat obesity is based on the development of compounds that assist in weight loss, being used safely and effectively for a long period. The endocannabinoid system is related to obesity, increasing orexigenic signs and reducing satiety signs. *In silico* evaluation through virtual screening and molecular modeling of *Cannabis sativa* phytocannabinoids for this purpose stems from their polypharmaceutical potential and the existence of synthetic cannabinoid drugs that have already shown this result. **Objective:** Perform virtual screening based on the phytocannabinoid pharmacophore of *C. sativa*, to search for anti-obesity agents with the potential to interact with the cannabinoid receptor 1 (rCB1). **Methodology:** The virtual screening included the prediction of biological activity, the evaluation of the physico-chemical, pharmacokinetic and toxicological properties of cannabinoids (to obtain a reference pharmacophore) and ZINC molecules, as well as molecular docking in rCB1 (PDB: 5U09). **Results and discussion:** The pharmacophore obtained revealed a 5-point model, with a hydrogen acceptor region and four hydrophobic regions, and this was submitted to the ZINC server for virtual screening, where 78 molecules were obtained that signaled antagonistic activity on rCB1, in addition to anti-obesity activity. Among the ZINC molecules evaluated, after analysis of their physical-chemical, pharmacokinetic and toxicological profiles, the ZINC33053402 and ZINC19084698 pointed out as promising anti-obesity agents. **Conclusions:** The best profile of the ZINC molecules screened to act as an antagonist of rCB1 in peripheral anti-obesity activity were: ZINC33053402 and ZINC19084698 (for presenting a key bond for the blocking of the anandamide endocannabinoid agonist) and high GoldScore. In addition, these molecules have a possible factor favorable to the safety of using a cannabinoid antagonist at the peripheral level, due to their pharmacokinetic profile, which can overcome the barriers of adverse effects inherent to this pharmacological class.

Keywords: Molecular Docking; Structure-activity relationship; Natural cannabinoids; rCB1; Virtual Screening.

Acknowledgements: Laboratory of Pharmaceutical and Medicinal Chemistry (PharMedChem - UNIFAP), Department of Pharmaceutical Sciences (School of Pharmaceutical Sciences of Ribeirão Preto – USP) e Department of Chemistry (School of Philosophy, Sciences and Letters of Ribeirão Preto – USP).

1 INTRODUÇÃO

1.1 OBESIDADE

A obesidade é considerada pela organização mundial de saúde (OMS) uma doença epidêmica global (do tipo crônico não transmissível), sendo problema de saúde pública que vem crescendo anualmente acompanhado de comorbidades como diabetes mellitus, doenças cardiovasculares, acidente vascular cerebral, hipertensão e certos tipos de câncer (endometrial, mama, ovário, próstata, fígado, vesícula biliar, rim e cólon) (IBSEN; CONNOR; GLASS, 2017; WHO, 2017).

É caracterizada pelo acúmulo anormal ou excessivo de gordura, principalmente na região abdominal, que ocorre pelo desequilíbrio da entrada de alimentos e o gasto de energia. É medida através do índice de massa corporal (IMC), trazendo riscos à saúde a partir que a medida seja igual ou maior que 25 (sendo considerada acima do peso), e igual ou superior a 30 (com obesidade). A princípio era tratada como um problema característico de países de alta renda, mas demonstram o aumento também nos países de baixa e média renda, particularmente em suas áreas urbanas (HAWKINS; HORVATH, 2017).

A obesidade pode ser classificada quanto à causa etiológica, quanto à quantidade de gordura em excesso, quanto à característica anatômica do tecido adiposo, quanto à distribuição regional da gordura corporal e quanto à época de seu início, conforme o exposto a seguir (YONAHA, 2016):

- Quanto à causa etiológica, classifica-se em obesidade exógena e endógena. Na exógena, o excesso de gordura corporal advém do equilíbrio energético positivo entre a ingestão e a demanda energética e corresponde a cerca de 98% dos casos. E a endógena está relacionada às causas hormonais, decorrentes de alterações no metabolismo tireoidiano, hipotálamo-hipofisário, tumores e síndromes genéticas.
- Quanto à quantidade de gordura em excesso, divide-se em leve, moderada, elevada ou mórbida.

- Quanto à característica anatômica do tecido adiposo, divide-se em hiperplásica, onde há um elevado número de células adiposas no organismo; e hipertrófica, que está associada ao tamanho aumentado das células adiposas existentes.
- Quanto à distribuição regional da gordura corporal, a obesidade pode ser do tipo androide (ou maçã), onde o acúmulo de gordura concentra-se na região abdominal (tronco, pescoço e cintura escapular); ou ginecoide (também conhecida comopera) em que o acúmulo de gordura é predominante na parte inferior do corpo (quadril, glúteo e coxa superior).
- E quanto à época do início, pode ser progressiva, em que o aumento da gordura é gradual e se inicia desde a infância até a idade adulta; ou fase adulta, com início do acúmulo de gordura corporal na fase adulta e de característica hipertrófica.

1.2 EPIDEMIOLOGIA

Os dados mais recentes da OMS expõem que de 1975 a 2016 a obesidade quase triplicou, chegando a 1,9 bilhões de adultos (população com idade acima de 18 anos) com excesso de peso, e dentre estes 650 milhões são obesos. Dentre as crianças (menores de 5 anos), haviam 41 milhões acima do peso, e na faixa etária dos 5 aos 19 anos mais de 340 milhões (WHO, 2017).

No Brasil a obesidade cresceu, num período de dez anos, 60%, onde em 2006 tinha índices de 11,8% e em 2016 alcançou 18,9% da população do país. A frequência é semelhante em homens e mulheres, a prevalência duplica a partir dos 25 anos de idade, e quanto menor o grau de escolaridade maior a prevalência (VIGITEL BRASIL, 2016).

1.3 TRATAMENTOS FARMACOLÓGICOS

Há três principais formas de tratamento para a obesidade: mudanças no estilo de vida, cirurgia bariátrica e medicamento. Diante dos riscos inerentes à obesidade, a cirurgia bariátrica tem se mostrado como alternativa efetiva na perda de peso e redução da morbi-mortalidade relacionada a esta doença. No entanto, por ser invasiva, de alto custo e por não ser aplicada a todos os perfis de obesidade, não é

um tratamento comum nem de primeira escolha. A terapia medicamentosa é indicada para aqueles cuja necessidade de perda de peso não pode ser superada apenas com mudanças nutricionais (LEWIS et al., 2017).

Basicamente, há dois grupos de medicamentos inibidores de apetite: os catecolaminérgicos e os serotoninérgicos. Os primeiros atuam liberando noradrenalina dos grânulos sinápticos, mas por causarem dependência devem ser usados por períodos curtos de até 12 semanas. Já os serotoninérgicos agem pela recaptação da serotonina (YONAHA, 2016).

Dentre os fármacos antiobesidade mais comercializados, tem-se o orlistat (inibidor da lípase pancreática) e a sibutramina (inibidor da recaptação de noradrenalina e serotonina). O perfil de eficácia e segurança do orlistat e da sibutramina foi avaliado e aprovado, mas ambos exercem um efeito modesto na perda de peso, com efeitos adversos leves. O orlistat desencadeia efeitos colaterais gastrointestinais, enquanto a sibutramina desencadeia hipertensão, dores de cabeça, insônia, boca seca, náusea e vômitos, tontura e palpitações (SRIVASTAVA; LAKHAN; MITTAL, 2007).

Outros agentes serotoninérgicos (agentes antidepressivos como a sertralina, fluoxetina e bupropiona) são utilizados como terapia auxiliar no intuito de reduzir sintomas da ansiedade e depressão (YONAHA, 2016).

Atualmente, a busca por novos alvos para o tratamento da obesidade motiva pesquisas mundialmente. Como exemplo disso, o rimonabanto (antagonista canabinoide) chegou a ser comercializado na Europa, mas por causar efeitos colaterais em nível de Sistema Nervoso Central (SNC), foi descontinuado (COLON-GONZALEZ et al., 2013).

1.4 SISTEMA ENDOCANABINOIDE (SECB)

O Sistema endocanabinoide (SECB) envolve a presença dos seguintes componentes: receptores canabinoides (rCB), canabinoides endógenos (ou endocanabinoides - ECs), e enzimas envolvidas na síntese e degradação dos endocanabinoides (ROMERO-ZERBO; BERMÚDEZ-SILVA, 2014).

Os receptores canabinoides pertencem à superfamília de proteínas G (proteínas triméricas de subunidades α e βγ), as quais são caracterizadas por apresentar 7 domínios transmembranares, um terminal extracelular NH_2, e um

terminal intracelular COOH, e encontram-se distribuídos ao longo do corpo humano (AKBAS et al., 2009).

Na espécie humana, foram identificados dois receptores canabinoides, nomeados como CB1 e CB2. Receptores CB1 regulam principalmente a neurotransmissão no SNC, mas também se encontram presentes perifericamente em órgãos gastrointestinais, tecido adiposo, miocárdio, endotélio vascular, nervos periféricos, fígado, pâncreas e músculo esquelético (SZABO et al., 2014). É estudado como alvo para várias doenças, como dor, ansiedade, esclerose múltipla, obesidade, doenças de Huntingnton e Parkinson. Já os receptores CB2 regulam respostas imunes e inflamatórias, e tem sido relacionado como alvo em distúrbios inflamatórios periféricos, como a nefrotoxicidade (FRAGUAS-SÁNCHEZ; FERNÁNDEZ-CARBALLIDO; TORRES-SUÁREZ, 2014). Um terceiro receptor menos estudado, CB3, é relatado por Paulo e Abreu (2015), onde está possivelmente relacionado à ativação de receptores vaniloides.

Os rCB apresentam ligantes endógenos conhecidos, com ação neuromoduladora, pertencentes a uma família de lipídeos e que tem estrutura química diferente do ligante exógeno tetrahidrocanabinol (THC). Os ECs mais importantes são araquidonoil etanolamida (ou anandamida - AEA) e o 2-araquidonoilglicerol (2-AG) (IBSEN; CONNOR; GLASS, 2017; MARCIA et al., 2017).

Tanto a AEA como a 2-AG têm ação sobre rCB1 ligeiramente superior à rCB2, sendo 2-AG mais eficaz, ligando-se como agonista parcial em ambos os tipos de receptores (ROMERO-ZERBO; BERMÚDEZ-SILVA, 2014). Ao interagir com os receptores canabinoides são capazes de desencadear, de modo fisiologicamente controlado, efeitos biológicos tal quais os desencadeados por canabinoides exógenos, sendo agonistas deste receptor (ELSOHLY, 2007).

O mecanismo de ativação do rCB1 varia de acordo com a sua localização. Se pré-sináptica ocorrerá pela inibição da adenilato ciclase, gerando hiperpolarização com a consequente diminuição na liberação de neurotransmissores. Se pós-sináptica, a ação dos rCB1 está na regulação dos canais de K^+ e inibição da adenilato ciclase. Já mecanismo de ativação de CB2 ocorre pela inibição da adenilato ciclase e ativação da proteína quinase ativada por mitógeno (MAPK) (MARCIA et al., 2017; MILANO; TECCE; CAPASSO, 2017).

A ação neuromoduladora dos ECs é decorrente das seguintes características, presentes principalmente em AEA e 2-AG: apresentam vias sintéticas distintas, sua

liberação das células ocorre após a despolarização da membrana e a entrada de cálcio; e sua ação é terminada com sua recaptação e degradação por uma enzima intracelular, a amida hidrolase de ácidos graxos (HAWKINS; HORVATH, 2017).

1.5 SECB E A OBESIDADE

Com relação ao desencadeamento da obesidade, o SECB pode atuar de dois modos no SNC, onde o primeiro ocorre via sistema mesolímbico, atuando no incentivo a procura por alimentos palatáveis (com capacidade de proporcionar prazer); e o segundo é via hipotálamo, onde, sob demanda, modula o apetite ao regular a liberação de substâncias orexígenas ou anorexígenas (GODOY-MATOS et al., 2006). Basicamente, a sinalização EC no hipotálamo consiste em modular a alimentação pela diminuição dos sinais de saciedade e aumento dos sinais orexígenos. Esta sinalização pode ser observada após o jejum, quando os ECs se tornam ativados no hipotálamo, estimulando o apetite (BURDYGA et al., 2004; SRIVASTAVA; LAKHAN; MITTAL, 2007; ENGELI et al., 2014;).

Engeli et al. (2014) expõem a relação de rCB1 com a obesidade, realizando estudo de avaliação dos ECs em jejum e após a ingestão de alimentos em humanos obesos e normais, submetidos a duas semanas de dieta isocalórica baixa e rica em gordura. Nesse estudo, ficou evidenciado que a AEA basal de obesos era significantemente alta, enquanto os níveis de 2-AG foram semelhantes aos dos indivíduos normais, associando, então, o SECB à patogênese da doença metabólica, onde o rCB1 modula os tecidos pancreático, adiposo, músculo esquelético e metabolismo do fígado. Burdyga et al. (2004) relatam que rCB1 estão expressos em maior quantidade durante o jejum, enquanto a ingestão alimentar promove a diminuição destes receptores.

Em virtude dessas informações comprovou-se que o bloqueio do rCB1 reduz o peso corporal em animais por ações centrais e periféricas (ENGELI et al., 2014). A sinalização canabinoide mostrou que o bloqueio dos rCB1 permitiu controlar a termogênese e a atividade endócrina do tecido adiposo, sugerindo a indução de um balanço energético negativo. Mas, no que diz respeito aos antagonistas canabinoides, estudos clínicos revelaram que o efeito de rimonabanto e taranabanto quanto a perda de peso não excedeu a obtida com outros fármacos antiobesidade

atualmente aprovados e comercializados, além de ter efeitos adversos psiquiátricos potencialmente graves que limitam seu uso clínico (DESPRÉS, 2008)

Després (2008) relaciona os ECs com a fisiopatologia dos transtornos alimentares, sendo capazes de modular a ingestão alimentar em animais e humanos. Isto está intimamente ligado ao fato de os rCB1 serem altamente expressos em áreas do SNC envolvidas com o sistema de recompensa (hipotálamo, núcleos arqueados e paraventriculares) e também com a presença periférica de rCB1 no sistema nervoso entérico, o que explica a coordenação da sinalização com os receptores presentes no SNC bem como a possibilidade de regulação da alimentação a nível periférico.

A AEA, como EC intestinal, em resposta a um período de jejum de 24 horas, apresenta-se em concentrações aumentadas no intestino delgado de ratos, retornando aos níveis normais após a ingestão de alimentos, sendo, portanto, um sinal relativo à fome. A relação entre o aumento da concentração de AEA e rCB1 foi demonstrada em experimento com a administração intraperitoneal de agonista rCB1 em ratos parcialmente saciados, onde houve o estímulo da ingestão alimentar, e com a administração periférica do antagonista canabinoide rimonabanto, o qual exerceu efeito redutor da ingestão de alimentos tanto nos ratos parcialmente saciados, como naqueles que se encontravam em jejum (HAWKINS; HORVATH, 2017).

Associando o SECB e os receptores canabinoides à fisiopatologia da obesidade tem-se o excesso de ECs sem necessariamente haver aumento na expressão de rCB1, indicando uma nova via de ação farmacológica antiobesidade sobre a redução da concentração destes, levando à regulação da ingestão de alimentos e possivelmente também do gasto de energia (DESPRÉS, 2008). Portanto, tendo função conhecida, a ativação da sinalização de rCB1, por AEA, estimula o apetite, enquanto o seu bloqueio por um antagonista canabinoide induz a supressão do apetite (AKBAS et al., 2009).

O SECB é bem conhecido por sua relação com a regulação da ingestão de alimentos e metabolismo da gordura, estando aumentado na obesidade humana, e tendo no rCB1 o principal modulador da sinalização, tanto em nível central, como perifericamente. Receptores CB1 nos terminais GABAérgicos da área tegumentar ventral aumentam a atividade dopaminérgica neuronal, aumentando a liberação de dopamina no núcleo accumbens, a qual leva ao aumento do consumo de alimentos.

Perifericamente, a ativação de CB1 regula o balanço energético ao estimular o armazenamento de lipídeos e triglicerídeos e por desencadear mecanismos lipogênicos (aumenta a atividade da lipoproteína lipase) (FRAHER et al., 2015). Portanto, o bloqueio de tal receptor por antagonistas, no tecido adiposo, diminui o armazenamento de gordura através da diminuição da concentração dos ácidos graxos livres. rCB1 também está relacionado à diminuição dos movimentos peristálticos, que prolongam o tempo de trânsito intestinal, promovendo ganho de peso. Porém, sua capacidade de modular a ingestão de alimentos também pode influenciar a ação orexígena, ou seja, estimular o apetite através da ligação agonista ao rCB1 (GODOY-MATOS et al., 2006).

Ao ativar receptores canabinoides centrais, os ECs estão relacionados ao aumento da ingestão de alimentos e ao ganho de peso em animais (AKBAS et al., 2009). A sobrerregulação, ou seja, ativação do sistema canabinoide pode causar acúmulo excessivo de gordura visceral, redução dos níveis de adiponectina (adipocina associada à redução do acúmulo de lipídios), hiperglicemia e dislipidemia (FRAHER et al., 2015).

Akbas et al. (2009) ratificam que os antagonistas dos rCB1 podem atuar tanto em nível central como perifericamente. Os de localização central, ao serem ativados, relacionam-se a um efeito anorexígeno, modulação da liberação de hormônios no hipotálamo e reduz a motivação para ingestão de alimentos palatáveis no núcleus accumbens. Perifericamente, há estimulação de sinais anoréticos por rCB1 do trato gastrintestinal, inibição de enzimas lipogênicas no tecido adiposo, diminuiçãoda lipogênese e inibição da esteatose no fígado, aumentando níveis de adiponectina e aumentando a captação de glicose e consumo de oxigênio nos músculos para aumentar a termogênese.

O rCB1 já é validado como alvo para o tratamento da obesidade, mas também para o tratamento de doenças hepáticas, síndrome metabólica e dislipidemias. No entanto, os efeitos colaterais adversos apresentados pelo rimonabanto (primeiro fármaco antagonista rCB1 comercializado), tais como depressão e ansiedade, o levaram a ser descontinuado, e consequentemente este fato levou ao encerramento dos estudos clínicos de outros antagonistas rCB1 que estavam em andamento (taranabanto, otenabanto e ibipinabanto). Atualmente, moléculas naturais vêm sendo estudadas para este fim, buscando maior segurança ao evitar os efeitos sobre o SNC (SRIVASTAVA; LAKHAN; MITTAL, 2007). A

presença de rCB1 no SNC atrai o foco de pesquisadores para o desenvolvimento de ligantes seletivos com perfis favoráveis e seguros, de modo a evitar a ativação de múltiplas vias de sinalização no cérebro, as quais estão relacionadas a eventos adversos (ROMERO-ZERBO; BERMÚDEZ-SILVA, 2014).

1.6 *Cannabis sativa* E FITOCANABINOIDES

Os canabinoides são terpenosfenóis típicos de *C. sativa* (também chamados de fitocanabinoides). Apresentam 21 carbonos em sua estrutura química e estão divididos em onze subclasses, as quais abrangem seus metabólitos, derivados e produtos de transformação. São elas: canabigerol (CBG), canabicromeno (CBC), canabidiol (CBD), delta-9-tetrahidrocanabinol (Δ^9-THC), delta-8-tetrahidrocanabinol (Δ^8-THC), canabiciclol (CBL), canabielsoina (CBE), canabinol (CBN), canabinodiol (CBDN), canabitriol (CBT) e canabinoides diversos (PERTWEE, 2014). Dentre estes há os que são psicoativos (Δ^9-THC) e os que são não psicoativos (as demais classes) (PAULO; ABREU, 2015).

Os primeiros estudos fitoquímicos revelaram inicialmente que a constituição fitoquímica de *C. sativa* possuía 483 compostos, sendo dentre estes 66 canabinoides elucidados (ELSOHLY, 2007). Atualmente, com a intensificação de pesquisas, a quantidade de compostos identificados aumentou, chegando a 565 compostos, com 120 canabinoides evidenciados, isolados ou relatados (ELSOHLY, 2017).

O uso etnofarmacológico de *C. sativa* originalmente esteve associado a rituais religiosos, dentro das indústrias de papel e construção. Sofreu desprezo quanto ao uso medicinal, por ter se destacado por seus efeitos psicoativos, ganhando status de droga ilícita, mas, atualmente, destaca-se pelo seu potencial polifarmacêutico, tendo estudos fitoquímicos bem elucidados e testes laboratoriais para diversas finalidades terapêuticas (MARCIA et al., 2017).

1.7 MODELAGEM MOLECULAR

A docking molecular avalia a ligação de uma molécula à estrutura de um receptor, analisando as características químicas que se relacionam com a ligação.

Busca-se então a molécula com maior afinidade de ligação pelo sítio ativo, apresentando o maior número de interações (FONSECA et al., 2013).

A triagem virtual é um processo que avalia o acoplamento de várias moléculas a um sítio ativo, analisando sua afinidade pelo sítio ativo de uma enzima, seja por inibição ou por indução. O resultado final da triagem virtual é demonstrado por um ranking dos compostos, onde os compostos que apresentarem as maiores interações energética terão boas possibilidades de atuarem sobre o sítio ativo (HODAVANCE et al., 2016; ZLEBNIK; CHEER, 2016).

Porém, o processo de análise de modelagem molecular envolve, antes de reconhecer como viável a interação de um ligante a um sítio ativo, se os compostos terão atividade biológica para o alvo escolhido, via busca comparativa em servidores online; avaliar as suas propriedades físico-químicas (que ditam a biodisponibilidade via oral) e as variáveis farmacocinéticas que afetam a capacidade do composto de atingir seu alvo e posteriormente ser adequadamente metabolizado e eliminado do organismo (prevendo sua absorção, distribuição, metabolismo e excreção), e toxicológicas (tais como carcinogenicidade e mutagenicidade) que devem ser superadas para assegurar que o ligante de fato chegue ao sítio ativo e ocupe-o de forma segura e eficaz.

Portanto, considerando a relação existente entre o SECB e a obesidade, bem como a existência de canabinoides sintéticos desenvolvidos para o tratamento da obesidade e a busca ativa pelo desenvolvimento de novas alternativas de tratamento para esta doença, esta pesquisa visou trabalhar a modelagem molecular dos canabinoides de *C. sativa* no sítio ligante do rCB1, no intuito de investigar a viabilidade destes compostos químicos como ligantes para este alvo a nível periférico, no qual, poderão modular negativamente a ativação do sistema endocanabinoide, bem como realizar triagem virtual baseada no farmacóforo dos fitocanabinoides para a busca de novas moléculas promissoras para o tratamento da obesidade.

2 OBJETIVOS

2.1 OBJETIVO GERAL

Identificar compostos com atividade antiobesidade através de triagem virtual baseada em fitocanabinoides.

2.2 OBJETIVOS ESPECÍFICOS

a) Prever, *in silico,* a atividade biológica dos compostos químicos estudados;
b) Construir o modelo farmacofórico dos canabinoides estudados;
c) Predizer as propriedades farmacocinéticas e toxicológicas dos canabinoides selecionados;
d) Determinar, através de docagem molecular, os canabinoides que tenham interação antagonista no receptor canabinoide 1;
e) Realizar triagem virtual baseada em farmacóforo para a obtenção de novos agentes antiobesidade.

Submetido para publicação para revista ChemMedChem.

Virtual screening based on phytocannabinoids for anti-obesity activity

Lenir C. Correia[a], Jaderson V. Ferreira[a], Henrique B. de Lima[a], Guilherme M. Silva[b,c], Carlos H. T. P. da Silva[b,c], Lorane I. S. Hage-Melim*[a]

[a] B.S.Lenir C. Correia, MSc.Jaderson V. Ferreira, Henrique B. de Lima, Dr. Lorane I. da S. Hage-Melim, https://orcid.org/0000-0002-7851-7363
Laboratory of Pharmaceutical and Medicinal Chemistry (PharMedChem)
Federal University of Amapá, Rod. JK, Km 02, Macapá (Brazil)
E-mail:loranehage@gmail.com; lorane@unifap.br
[b] Dr. C. H. T. P. da Silva, MSc. G. M. Silva
Department of Pharmaceutical Sciences
School of Pharmaceutical Sciences of Ribeirão Preto, University of São Paulo, Ribeirão Preto (Brazil)
[c] Dr. C. H. T. P. da Silva, MSc. G. M. Silva
Department of Chemistry
School of Philosophy, Sciences and Letters of Ribeirão Preto, University of São Paulo, Ribeirão Preto (Brazil)

Abstract: Search for new pharmacological alternatives for obesity is based on the design and development of compounds that can aid in weight loss, so that they can be used safely and effectively over a long period, while maintaining their function. The endocannabinoid system is related to obesity by increasing orexigenic signals and reducing satiety signals. *Cannabis sativa* is a medicinal plant of polypharmaceutical potential that has been widely studied for various medicinal purposes. The *in silico* evaluation of their natural cannabinoids (also called phytocannabinoids) for anti-obesity purpose stems from the existence of synthetic cannabinoid compounds that have already presented this result, but which did not guarantee patient safety. In order to find new molecules from *C. sativa* phytocannabinoids, with potential to interact with the pharmacological target cannabinoid receptor 1, a pharmacophore-based virtual screening was performed, including the evaluation of physicochemical, pharmacokinetic, toxicological predictions and molecular docking. The results obtained from the ZINC[12] database pointed to ZINC33053402 and ZINC19084698 molecules, as promising anti-obesity agents.

Introduction

Obesity is considered a global epidemic disease, being a public health problem that has been growing annually, according to the World Health Organization (WHO). It may lead to comorbidities such as diabetes mellitus, cardiovascular disease, stroke, hypertension and certain types of cancer (endometrial, breast, ovarian, prostate, liver, gallbladder, kidney and colon).[2,19]

Currently, the search for new targets for the treatment of obesity motivates research worldwide. An example of this was rimonabant, a cannabinoid antagonist that was marketed in Europe, but it was discontinued because presented several side effects on the central nervous system (CNS).[20]

The endocannabinoid system involves the presence of the following components: cannabinoid receptors (rCB), endogenous cannabinoids (endocannabinoids), and enzymes involved in endocannabinoid synthesis and degradation.[6] Cannabinoid receptors belong to the G protein superfamily and are distributed throughout the human body.[7] rCB1 primarily regulate central nervous system (CNS) neurotransmission, but are also present peripherally in gastrointestinal organs, adipose tissue, myocardium, vascular endothelium, peripheral nerves, liver, pancreas, and skeletal muscle.[8] It has been studied as a target for various diseases such as pain, anxiety, multiple sclerosis, Huntingnton and Parkinson's diseases, and even for obesity.

The rCB1 are known for having endogenous neuromodulatory ligands that belong to the family of lipids, which present different chemical structure than the exogenous tetrahydrocannabinol (THC) ligand. Among the most important endogenous cannabinoid (ECs) neurotransmitter are arachidonoyl ethanolamide (or anandamide - AEA), [2,10] being agonists of such receptor.[11]

The activation mechanism of rCB1 varies according to its location. If it is presynaptic and with adenylate Cyclase inhibition, it may be generated hyperpolarization with consequent decrease in neurotransmitter release. If it is postsynaptic, the action of rCB1 is on K^+ channel regulation and adenylate cyclase inhibition.[10,12]

The neuromodulatory action of AEA is due to the following characteristics: they have distinct synthetic pathways; their cell release occurs after membrane depolarization and calcium intake; and its action is terminated with its reuptake and degradation by an intracellular enzyme (fatty acid amide hydrolase).[4]

Regarding the onset of obesity, the AEA can act by two different ways in the CNS. The first occurs via the mesolimbic system, acting to encourage the search for palatable foods (capable of providing pleasure); and the second is trougth the hypothalamus, where modulates appetite by regulating the release of orexigenic or anorectic substances.[13] Basically, EC signaling in the hypothalamus consists of modulating feeding by decreasing satiety signals and increasing orexigenic signals. This signaling can be observed after fasting, when ECs become activated in the hypothalamus, stimulating appetite.[1,14,15]

Engeli and collaborators[14] expose the relationship between rCB1 and obesity by conducting a study of fasting ECs and after eating foods in obese and normal humans, submitted to two weeks of low-fat, high-isocaloric diet. In this study, it was evidenced that the basal AEA of obese was significantly high, while the levels of 2-AG (other endocannabinoid) were similar to those of normal individuals, thus associating endocannabinoid system with the pathogenesis of metabolic disease, where rCB1 modulates pancreatic, adipose, skeletal muscle and liver metabolism. Burdyga and collaborators[15] report that rCB1 are expressed in greater amounts during fasting, while food intake promotes the decrease of these receptors.

Typical terpenosphenols of *C. sativa* are called phytocannabinoids. They have 21 carbons in their chemical structure and are divided into eleven subclasses, which include their metabolites, derivatives and transformation products. They are: cannabigerol (CBG), cannabichromene (CBC), cannabidiol (CBD), delta-9-tetrahydrocannabinol (Δ9-THC), delta-8-tetrahydrocannabinol (Δ8-THC), cannabicyclol (CBL), cannabielsoin (CBE), cannabinol (CBN), cannabinoidiol (CBDN), cannabitriol (CBT) and various cannabinoids.[16] Among these are those that are psychoactive (Δ9-THC) and those that are non-psychoactive (the other classes).[17]

In this way, considering the mentioned works that evaluated the relationship between endocannabinoid system and obesity, as well as the existence of synthetic cannabinoids developed for the treatment of obesity, and also the intense search for the development of new treatment alternatives for such disease, this article aimed to perform a molecular modeling study of phytocannabinoids of *C. sativa* to provide new promising molecules with interest in the treatment of obesity.

Results and Discussion

Chemical structure and biological activities prediction of phytocannabinoids

Cannabinoid molecules evaluated in this study were designed based on the work of Pertwee in the *Handbook of Cannabis*.[16] Of the 104 initial phytocannabinoids, only 41 showed a prediction of activity for rCB1 antagonism, and their chemical structures are presented in Figure 1.

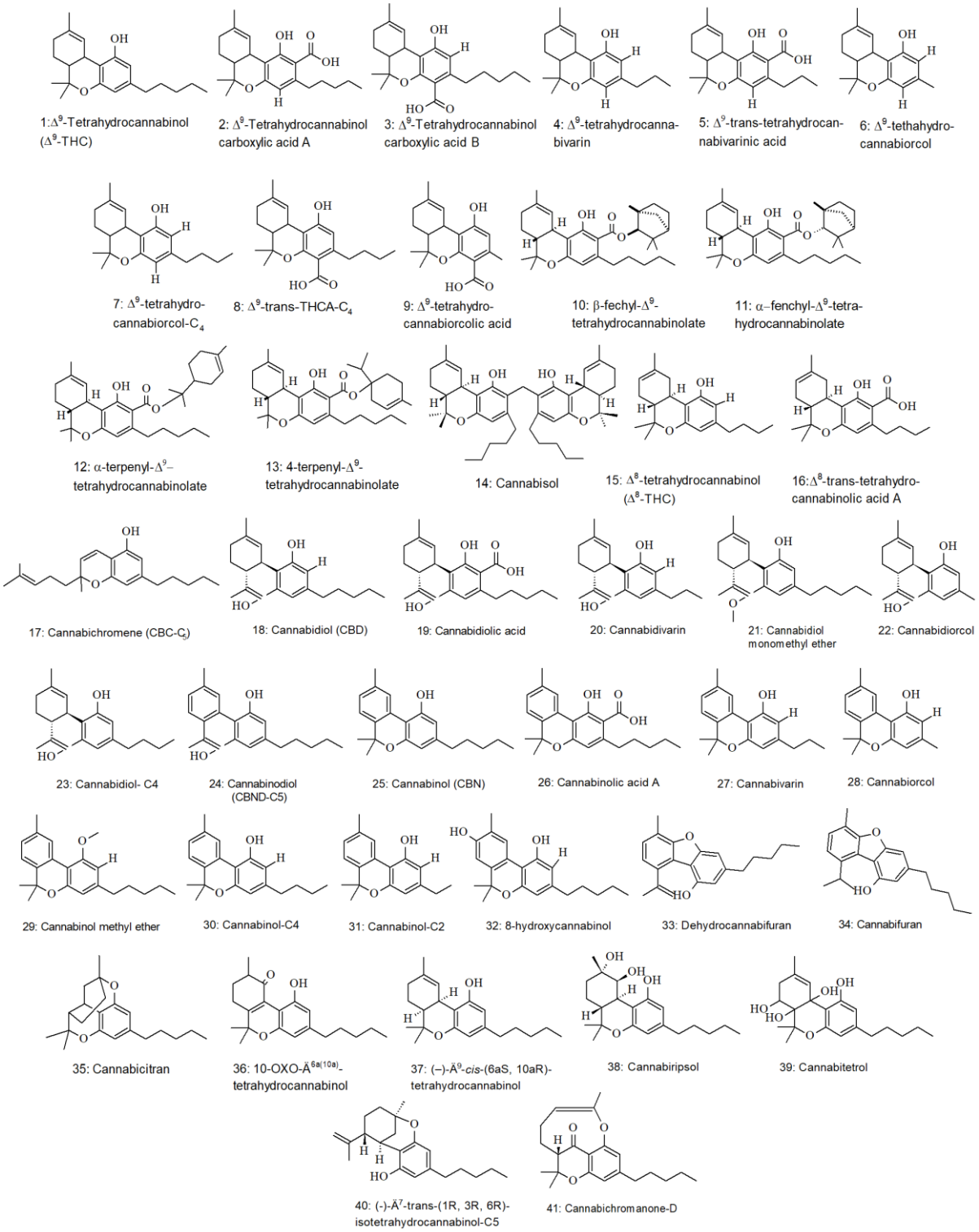

Figure 1. Representation of chemical structures of 41 phytocannabinoids present in *C. Sativa* with rCB1 antagonism activity**.**

Table 1. Values of P_a and P_i, regarding biological activities predicted on the PASS server, of 41 phytocannabinoids with $P_a > P_i$ for cannabinoid antagonist activity.

Phytocannabinoid	RCB1 antagonism		Phytocannabinoid	RCB1 antagonism	
	P_a[a]	P_i[b]		P_a[a]	P_i[b]
Rimonabant	**0.959**	**0.001**	21	0.171	0.004
01	**0.513**	**0.002**	22	0.168	0.004
02	0.125	0.005	23	0.201	0.004
03	0.132	0.005	24	0.057	0.021
04	0.394	0.003	25	0.303	0.003
05	0.082	0.011	26	0.052	0.024
06	**0.409**	**0.003**	27	0.224	0.004
07	**0.470**	**0.002**	28	0.240	0.004
08	0.112	0.006	29	0.273	0.003
09	0.109	0.006	30	0.273	0.003
10	0.039	0.037	31	0.235	0.004
11	0.039	0.037	32	0.173	0.004
12	0.065	0.017	33	0.040	0.036
13	0.071	0.014	34	0.044	0.031
14	0.258	0.004	35	0.087	0.010
15	**0.623**	**0.002**	36	0.045	0.029
16	0.117	0.004	**37**	**0.513**	**0.002**
17	0.046	0.029	38	0.064	0.018
18	0.231	0.004	39	0.041	0.034
19	0.042	0.034	40	0.050	0.026
20	0.153	0.005	41	0.049	0.026

[a] Probability of activity. [b] Probability of inactivity.

The PASS server has been used to predict the biological activy for initial 104 molecules, in terms of P_a (probability of being active) and P_i (probability of being inactive). Table 1 shows that 41 of them showed positive indicative results for antagonist activity on rCB1 receptor (Pa > Pi), and the others showed no indication of biological activity. In order to search for a common pharmacophore in between them, in the next step, only 32 molecules (maximum limit of molecules accepted by servidor) with the best results were used: 01, 02, 03, 04, 05, 06, 07, 08, 09, 12, 13, 14, 15, 16, 18, 20, 21, 22, 23, 24, 25, 26, 27, 28, 29, 30, 31, 32, 35, 37, 38, e 40. The most relevant results were those with Pa > 0.4, highlighted in bold in Table 1.

Pharmacophoric pattern of phytocannabinoids with prediction of antagonist activity on rCB1

Determination of regions on molecule structures that are most likely related with their biological activity, i.e. derivation of their pharmacophoric patterns, was performed on the PharmaGist server[21] with the 32 best sorted molecules in the previous step. Alignment of such molecules presented the best score of 15.993 with the following points in pharmacophoric pattern: 01 hydrogen-accepting region (HBA) (yellow sphere) and 04 hydrophobic regions (HPO) (green spheres) (Figure 2).

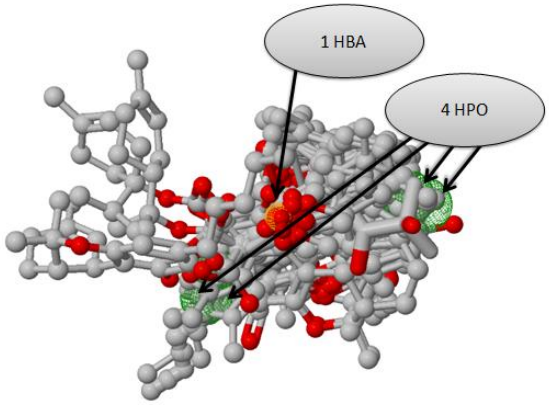

Figure 2. Pharmacophoric pattern containing five points obtained by alignment 32 molecules with the best potential antagonist over rCB1.

Sharma and collaborators[22] defined as a characteristic pharmacophore of peripheral-acting rCB1 antagonists a four-point model with the following regions: 1 HBA, 1 HPO and 2 aromatics (AR). In the same study, other pharmacophoric hypotheses were evaluated, including a five-point model with: 1 HBA, 2 HPO and 2 AR. Wang and collaborators[23] also obtained two 5-point pharmacophoric patterns where the first comprised 1 HBA, 2 AR and 2 HPO; while the second 1 HBA, 1 AR and 3 HPO. The information shows us that there is no defined pharmacophoric pattern for cannabinoid antagonists.

The pharmacophoric pattern obtained in this study resembles Wang's second model, except for the aromatic region. However, it is noteworthy that the pharmacophoric patterns obtained in the literature, concerning cannabinoid antagonists, were built using individual molecules as reference, and do not refer to the alignment of various antagonists. The proposition of a novel pharmacophore may prove useful in the search for safer cannabinoid antagonists for anti-obesity activity.

Virtual Screening

In order to perform a pharmacophore-based screening, we used our previously described pharmacophore (1 HBA and 4 HPO), by using the purchasable database from ZINCPharmer server and 1000 hits were obtained as results, with RMSD ranging from 0.40 to 0.88Å.[24]

Subsequently, these hits were submitted to biological activity prediction on the PASS server. Results obtained showed that 78 molecules (Figure 3) were favorable to cannabinoid antagonist activity, besides presenting indicatives of anti-obesity activity, like Rimonabant, as shown in Table 2.

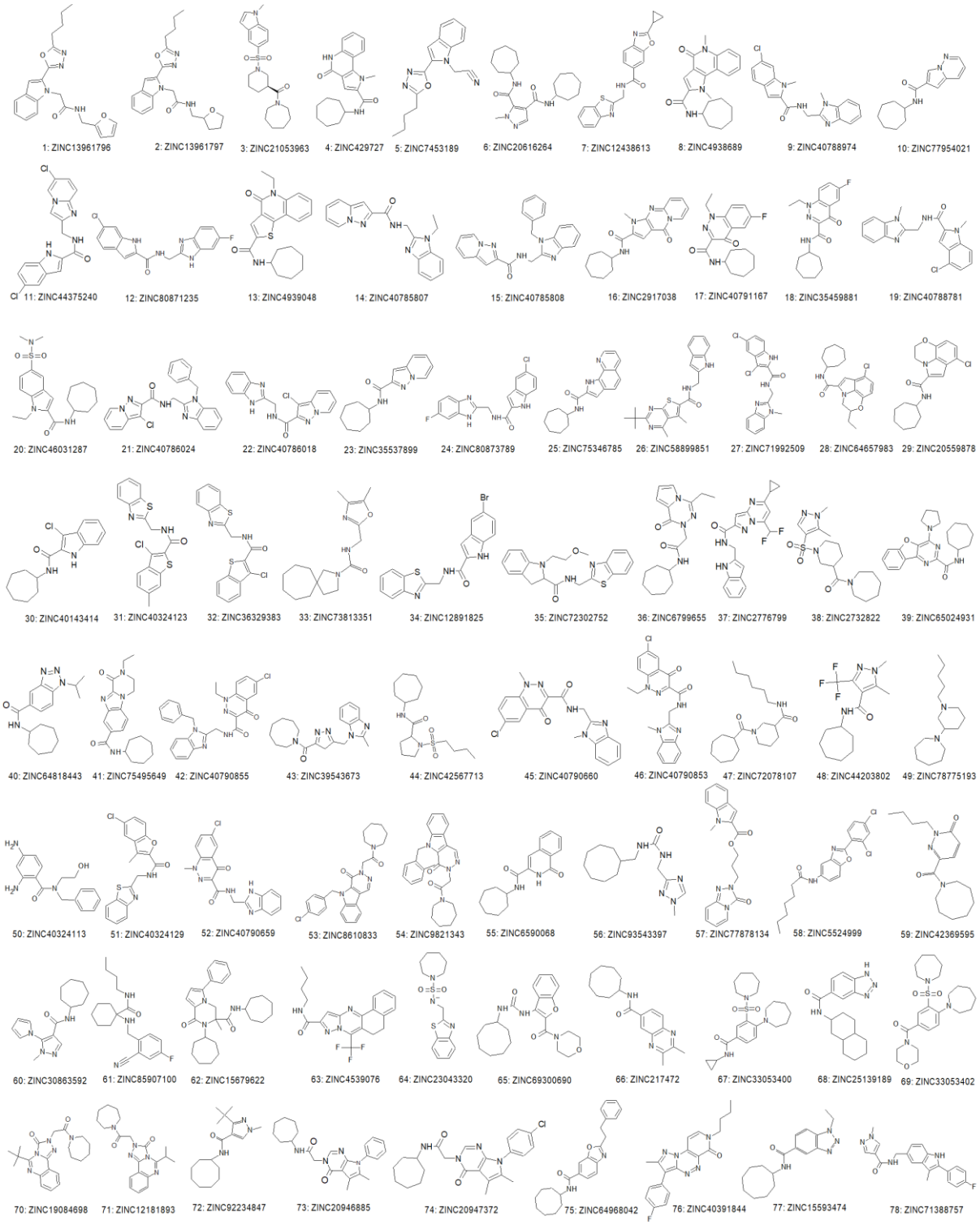

Figure 3. Representation of chemical structures of 78 ZINC molecules obtained as hits.

Table 2. Values of P_a and P_i, regarding biological activities predicted on the PASS server, of 78 ZINC molecules that showed activity prediction for rCB1 antagonism and anti-obesity.

Molecule	Zinc molecule	RCB1 Antagonist Activity		Anti-obesity Activity	
		Pa[a]	Pi[b]	Pa[a]	Pi[b]
Rimonabant	**ZINC1540228**	**0.959**	**0.001**	**0.805**	**0.005**
01	ZINC13961796	0.079	0.012	0.164	0.162
02	ZINC13961797	0.101	0.007	0.259	0.089
03	ZINC21053963	0.067	0.016	**0.711**	0.006
04	ZINC429727	0.043	0.032	0.271	0.082
05	ZINC7453189	0.115	0.006	0.169	0.156
06	ZINC20616264	0.075	0.013	**0.430**	0.033
07	ZINC12438613	0.041	0.034	0.231	0.104
08	ZINC4938689	0.076	0.013	0.326	0.059
09	ZINC40788974	0.144	0.005	0.341	0.054
10	ZINC77954021	0.077	0.013	0.351	0.051
11	ZINC44375240	0.072	0.014	0.299	0.069
12	ZINC80871235	0.049	0.026	0.271	0.082
13	ZINC4939048	0.046	0.029	0.202	0.124
14	ZINC40785807	0.053	0.024	0.369	0.046
15	ZINC40785808	0.063	0.018	0.299	0.069
16	ZINC2917038	0.050	0.025	0.178	0.146
17	ZINC40791167	0.103	0.007	**0.627**	0.010
18	ZINC35459881	0.069	0.015	0.371	0.046
19	ZINC40788781	0.179	0.004	**0.473**	0.025
20	ZINC46031287	0.120	0.005	**0.469**	0.026
21	ZINC40786024	0.061	0.020	**0.714**	0.006
22	ZINC40786018	0.055	0.022	**0.732**	0.005
23	ZINC35537899	0.206	0.004	**0.518**	0.019
24	ZINC80873789	0.052	0.024	0.290	0.073
25	ZINC75346785	0.058	0.021	0.268	0.084
26	ZINC58899851	0.142	0.005	0.213	0.116
27	ZINC71992509	0.038	0.038	0.394	0.040
28	ZINC64657983	0.131	0.005	**0.450**	0.029
29	ZINC20559878	0.216	0.004	**0.460**	0.027
30	ZINC40143414	0.102	0.007	**0.564**	0.014
31	ZINC40324123	0.051	0.025	0.321	0.061
32	ZINC36329383	0.062	0.019	0.359	0.049
33	ZINC73813351	0.048	0.028	0.361	0.049
34	ZINC12891825	0.095	0.008	**0.403**	0.038
35	ZINC72302752	0.106	0.007	0.332	0.056
36	ZINC06799655	0.046	0.029	0.270	0.078
37	ZINC02776799	0.042	0.033	0.163	0.163
38	ZINC02732822	0.062	0.019	**0.656**	0.008
39	ZINC65024931	0.081	0.011	0.268	0.084
40	ZINC64818443	0.059	0.021	0.189	0.135
41	ZINC75495649	0.049	0.027	0.308	0.065
42	ZINC40790855	0.080	0.012	**0.495**	0.022
43	ZINC39543673	0.137	0.005	**0.662**	0.008
44	ZINC42567713	0.054	0.023	0.323	0.060
45	ZINC40790660	0.053	0.024	**0.515**	0.019
46	ZINC40790853	0.081	0.011	**0.497**	0.021

47	ZINC72078107	0.107	0.007	0.277	0.079
48	ZINC44203802	0.121	0.005	**0.403**	0.038
49	ZINC78775193	0.069	0.015	0.229	0.105
50	ZINC40324133	0.051	0.025	0.262	0.087
51	ZINC40324129	0.050	0.025	0.301	0.068
52	ZINC40790659	0.040	0.036	**0.466**	0.026
53	ZINC08610833	0.090	0.009	0.230	0.104
54	ZINC09821343	0.048	0.028	0.171	0.153
55	ZINC06590068	0.042	0.033	0.181	0.143
56	ZINC93543397	0.069	0.016	0.395	0.040
57	ZINC77878134	0.044	0.031	0.247	0.095
58	ZINC05524999	0.112	0.006	0.261	0.088
59	ZINC42369595	0.160	0.004	0.220	0.111
60	ZINC30863592	0.086	0.010	0.348	0.052
61	ZINC85907100	0.124	0.005	0.289	0.073
62	ZINC15679622	0.052	0.024	0.243	0.097
63	ZINC04539076	0.179	0.004	0.214	0.115
64	ZINC23043320	0.080	0.012	**0.792**	0.005
65	ZINC69300690	0.104	0.007	0.208	0.119
66	ZINC00217472	0.082	0.011	0.281	0.077
67	ZINC33053400	0.070	0.015	**0.600**	0.012
68	ZINC25139189	0.043	0.032	0.247	0.095
69	ZINC33053402	0.123	0.005	**0.583**	0.013
70	ZINC19084698	0.163	0.004	**0.536**	0.017
71	ZINC12181893	0.066	0.017	0.362	0.048
72	ZINC92234847	0.076	0.013	0.222	0.109
73	ZINC20946885	0.053	0.024	0.337	0.055
74	ZINC20947372	0.129	0.005	**0.420**	0.034
75	ZINC64968042	0.061	0.019	0.263	0.087
76	ZINC40391844	0.083	0.011	0.382	0.043
77	ZINC15593474	0.066	0.017	0.164	0.162
78	ZINC71388757	0.067	0.016	0.194	0.130

[a] Probability of activity. [b] Probability of inactivity.

Overall, 78 molecules (or hits) obtained by virtual screening on the ZINC platform, showed positive predictions for anti-obesity activity, despite its low prediction for rCB1 antagonism. Of these, 24 had P_a results > 0.4, for anti-obesity activity, which are: 03, 06, 17, 19-23, 28-30, 34, 38, 42, 43, 45, 46, 48, 52, 64, 67, 69, 70 and 74.

Analysis of physicochemical properties

Physicochemical properties were evaluated according to Lipinski's Rule of Five (RO5),[25] which represents a fundamental guideline for getting to know the oral absorption of a drug candidate, regarding its permeability and solubility, as well as of what is necessary for pharmacological action. According to this, has good prediction for oral absorption those molecules that present results with at most a single violation of the evaluated parameters/properties, as follows: molecular weight (g/mol) (MW) ≤ 500, logP ≤ 5; hydrogen bond donors (HD) ≤ 5 and hydrogen bond acceptors (HA) ≤ 10.

The data required in analysis of 32 phytocannabinoids (the same selected for the pharmacophore derivation) was obtained from the Pubchem server. All of the 32 molecules evaluated at this stage, except molecule 14, showed results indicating good oral absorption (Table 3).

Table 3. Physicochemical properties of 32 phytocannabinoids obtained from the PubChem web server.

Phytocannabinoid	Molecular weight (g/mol)	LogP	Hydrogen Donors	Hydrogen Acceptors	Violations of the Rule of 5
Rimonabant	463.79	**6.1**	1	2	1
01	314.47	**7.0**	1	2	1
02	358.48	**7.0**	2	4	1
03	358.48	**6.5**	2	4	1
04	286.41	**5.9**	1	2	1
05	330.42	**6.0**	2	4	1
06	258.36	4.9	1	2	0
07	300.44	**6.4**	1	2	1
08	344.45	**6.0**	2	4	1
09	302.37	4.4	2	4	0
12	494.72	**8.5**	1	4	1
13	490.68	**9.2**	1	4	1
14	**640.95**	**11.6**	2	4	**2**
15	300.44	**5.2**	1	2	1
16	344.44	**7.73**	1	4	1
18	314.47	**6.5**	2	2	1
20	286.42	**5.4**	2	2	1
21	328.49	**6.8**	1	2	1
22	258.36	4.5	2	2	0
23	300.44	**6.0**	2	2	1
24	310.44	**7.0**	2	2	1
25	310.44	**6.1**	1	2	1
26	354.47	**6.2**	2	4	1
27	282.38	5.0	1	2	0
28	254.33	4.1	1	2	0
29	324.46	**6.4**	0	2	1
30	296.41	**5.6**	1	2	1
31	268.36	4.5	1	2	0
32	326.44	**5.8**	2	3	1
35	314.47	**5.9**	0	2	1
37	314.47	**7.0**	1	2	1
38	348.49	4.1	3	4	0
40	314.47	**6.4**	1	2	1

Bold results indicate violations of RO5.

According to the results presented in Table 3, only phytocannabinoid 14 violated RO5, with molecular weight and logP above the evaluated parameters, which indicates that its physicochemical profile does not favor its oral administration. The other molecules are in agreement with RO5 and also with the physicochemical characteristics of rimonabanto[26] in which the only violation is related to logP (equal to 6.11).

With regard to ability of a molecule to present good CNS permeability, the physicochemical property that is most related with this issue is the lipophilicity, which may be expressed by logP, i.e. the partition coefficient of a given molecule calculated in the system 1-octanol/water. With this in mind and taking into account a generic analysis in the context of RO5, values of logP ≤ 4 indicates that a molecule may be inactive in the CNS, and logP > 4 indicates that may be active in the CNS.[27] In view of this information, all phytocannabinoids presented in Table 3 have physicochemical potential to permeate the blood-brain barrier, an expected result for these metabolites that are known for their action in the CNS.

For the 78 ZINC molecules obtained from the virtual screening procedure, their physicochemical properties (Table 4) were collected from the ZINC server itself (http://zinc.docking.org/). All screened molecules were either within Lipinski's RO5.

Table 4. Physicochemical properties of 78 Zinc molecules obtained from the ZINC[12] web server.

Zinc molecules	Molecular weight (g/mol)	LogP	Hydrogen Donors	Hydrogen Acceptors	Violations of the Rule of 5
Rimonabant	463.79	**6.1**	1	2	1
01	378.432	2.9	1	7	0
02	382.464	2.6	1	7	0
03	403.548	3.0	0	6	0
04	337.423	3.5	2	5	0
05	280.331	2.9	0	5	0
06	360.502	3.8	2	6	0
07	349.415	3.0	1	5	0
08	351.45	4.0	1	5	0
09	352.825	3.4	1	5	0
10	257.337	3.0	1	4	0
11	359.216	3.9	2	5	0
12	342.761	3.4	3	5	0
13	368.502	**5.1**	1	4	1
14	319.368	2.4	1	6	0
15	381.439	3.6	1	6	0
16	338.411	3.3	1	6	0
17	331.391	1.8	1	5	0
18	256.349	3.6	1	3	0
19	352.825	3.3	1	5	0
20	391.537	3.7	1	6	0
21	415.884	4.2	1	6	0
22	325.759	2.5	2	6	0
23	257.337	3.3	1	4	0
24	342.761	**5.9**	3	5	1
25	307.397	4.0	2	4	0
26	392.528	5.0	2	5	0
27	373.243	3.9	2	5	0
28	360.885	**5.4**	1	4	1
29	332.831	4.6	1	4	0
30	290.794	4.6	2	3	0
31	372.902	4.9	1	3	0
32	358.875	4.5	1	3	0
33	319.449	3.8	1	5	0
34	386.274	3.9	2	4	0
35	365.458	3.2	1	5	0
36	316.405	2.3	1	6	0
37	381.386	3.4	2	6	0
38	368.503	1.4	0	7	0
39	378.476	4.3	1	6	0
40	300.406	3.7	1	5	0
41	354.454	2.9	1	6	0
42	471.948	3.5	1	7	0
43	351.454	2.8	0	6	0
44	330.494	3.1	1	5	0
45	381.823	1.6	1	7	0
46	395.85	1.9	1	7	0

47	336.52	4.8	1	4	0
48	303.328	3.3	1	4	0
49	252.446	4.1	0	2	0
50	370.861	4.7	1	4	0
51	356.834	4.3	1	4	0
52	367.796	1.5	2	7	0
53	448.954	4.7	0	6	0
54	428.536	4.4	0	6	0
55	284.359	3.6	2	4	0
56	279.388	2.1	2	6	0
57	350.378	2.7	0	7	0
58	391.298	**7.0**	1	4	1
59	291.395	2.8	0	5	0
60	286.379	2.7	1	5	0
61	331.435	3.9	2	4	0
62	461.65	**6.5**	1	5	1
63	388.393	4.6	1	5	0
64	325.459	2.4	1	5	0
65	399.491	4.1	2	7	0
66	311.429	4.3	1	4	0
67	419.591	3.7	1	6	0
68	298.39	3.3	2	5	0
69	449.617	2.9	0	7	0
70	381.48	3.5	0	7	0
71	367.453	2.8	0	7	0
72	291.439	4.4	1	4	0
73	392.503	3.5	1	6	0
74	426.948	4.2	1	6	0
75	376.5	**6.0**	1	4	1
76	351.385	4.6	0	6	0
77	300.406	3.8	1	5	0
78	362.408	3.3	2	5	0

Bold results indicate violations of RO5.

Regarding the potential to permeate the CNS according to logP values, the following molecules showed a possible poor permeability, with better results than rimonabant in the LogP parameter: 01-12, 14-20, 22-23, 25, 27, 33-38, 40-46, 48, 52, 55-57, 59-61, 64, 67-71, 73, 77 and 78. Other molecules that presented logP > 4, tend to show a higher CNS permeability, although such characteristic should be confirmed by further pharmacokinetic profile analysis.[27]

Lee and collaborators[28] presented the following physicochemical profile of cannabinoid antagonists: MW ≤ 500, logP ≤ 7; HD ≤ 3 and HA ≤ 6. It is noted that logP increases due to the fat-soluble profile of molecules that has CNS permeability characteristics, and the number of hydrogen donors and acceptors decreases. Evaluating phytocannabinoids through this prism it can be observed that molecule 14 would continue with 2 violations and that molecules 12, 13, 14 and 16 would violate the stipulated limit for logP. Evaluating ZINC molecules according to the physicochemical properties of cannabinoid antagonists, no molecule has more than a single violation.[28] It is noteworthy that the physicochemical profile of cannabinoid antagonists is inherent in the molecules that permeate the blood-brain barrier, a fact related to the adverse effects of this class of molecules and unwanted in this study.[26]

Pharmacokinetic properties analysis

The pharmacokinetic properties of phytocannabinoids are listed in Table 5 and were analyzed according to the parameters indicated in the QikProp manual. The evaluated parameters include: stars (similarity to known drugs: high: 0-2; medium: 3; and low: > 4), percentage of human oral absorption (% HOA) (high: > 80%; average: 25-80%; and low: <

25%), binding to human serum albumin (plogKhsa) (between -1.5 (low) and 1.5 (high)), pCaco-2 (intestinal cell) permeability (good: > 500 nm/sec; and poor: < 25 nm/sec) and pMDCK (renal cells) (good: > 500 nm/sec; and poor: < 25 nm/sec); plogBB (low permeation in blood-brain barrier when < -1 and easy permeation in blood-brain barrier when > -1) and Van der Waals surface area (PSA > 70: does not exceed BBB; PSA < 70 exceeds BBB).[29]

Table 5. Pharmacokinetic properties of 32 phytocannabinoids predicted and evaluated by the QikProp software.

	Similarity to known drugs	Absorption		Cellular Permeability		CNS distribution	
Phytocannabinoid	**Stars**	**% HOA**	**plogKhsa**	**pCaco-2 (nm/sec)**	**pMDCK (nm/sec)**	**plogBB**	**PSA**
Rimonabant	2	95	1.37	420	2697	1.48	30.2
01	3	100	1.22	4184	2324	-0.12	27.2
02	0	90	0.99	261	147	-0.80	68.1
03	0	97	0.73	188	103	-0.95	71.7
04	1	100	0.97	4190	2328	0.02	27.2
05	0	100	0.75	249	140	-0.65	68.2
06	1	100	0.73	4176	2319	0.17	27.2
07	1	100	1.09	4182	2322	-0.05	27.3
08	0	94	0.61	188	103	-0.86	71.6
09	0	88	0.29	176	96	-0.61	71.8
12	4	100	2.36	3665	2014	-0.39	47.5
13	4	100	2.42	4189	2327	-0.32	50.2
14	10	100	3.30	3217	1749	-0.80	49.9
15	1	100	1.08	4323	2408	-0.04	26.5
16	0	90	0.84	337	194	-0.61	64.7
18	1	100	1.02	2946	1590	-0.41	34.8
20	0	86	0.78	180	99	-1.10	35.9
21	3	100	1.23	6835	3950	0.04	21.9
22	1	100	0.54	2924	1577	-0.09	35.9
23	1	100	0.89	2943	1588	-0.33	34.8
24	1	100	0.89	2619	1401	-0.53	34.1
25	2	100	1.16	4228	2350	-0.13	26.9
26	0	91	0.91	309	177	-0.76	64.1
27	1	100	0.90	4225	2348	0.01	26.9
28	1	100	0.66	4230	2352	0.16	26.9
29	4	100	1.39	9906	5899	0.55	12.6
30	1	100	1.03	4237	2356	-0.06	26.9
31	1	100	0.78	4232	2352	0.09	26.9
32	0	100	0.89	1566	803	-0.65	47.8
35	3	100	1.31	6361	3655	0.13	15.7
37	3	100	1.22	4266	2373	-0.12	26.9
38	0	100	0.56	1027	509	-0.87	65.9
40	2	100	1.13	5535	3145	-0.06	25.0

%HOA: percentage of human oral absorption; QPlogKhsa: binding to human serum albumin; QPCaco: intestinal cells; QPMDCK: renal cells; QPlogBB: blood-brain barrier permeation; and PSA: Van der Waals surface area.

Prediction of binding to human serum albumin indicates the ability of the molecule to be absorbed and bioavailable to interact with its target receptor. Evaluating molecules from Table 5 in terms of plogKhsa, one can see that none showed low aggregation, 09 and 22 showed medium aggregation and others showed results that indicate high aggregation to serum albumin protein, similar result to rimonabant.

Blood-brain barrier permeation was assessed by plogBB (low permeation when < -1 and easy permeation when > -1)[30] and PSA (low brain permeation when > 70 Å).[31] Rimonabant showed a prediction for high permeability in the blood-brain barrier, a factor associated with its side effects. According to plogBB values obtained, only molecule 20 showed predictive results for low CNS permeation. On the other hand, according to PSA values obtained, molecules 03, 08 and 09 would have low CNS permeability. All other molecules tend to be well absorbed in oral administration and permeate the CNS due to their values of PSA < 70.[32] The best results, therefore, were for molecules 03, 08 and 09,

which had PSA> 70, despite medium cell permeability; and for molecules 01, 04, 06, 07, 15, 18, 21-25 and 27-40, with high cell permeability and prediction for action in the CNS.

Furthermore, we also predicted and evaluated pharmacokinetic properties of the 78 molecules selected from the virtual screening using the ZINC database, as can be seen in Table 6.

Table 6. Pharmacokinetic properties of 78 ZINC molecules predicted and evaluated in QikProp software.

	Similarity to known drugs	Absorption		Cellular Permeability		CNS distribution	
ZINC molecules	Stars	% HOA	plogKhsa	pCaco-2 (nm/sec)	pMDCK (nm/sec)	plogBB	PSA
Rimonabant	2	95	1.37	420	2697	1.48	30.2
01	0	100	0.15	1004	669	-0.73	79.9
02	0	100	0.06	1019	698	-0.72	79.3
03	0	100	-0.19	1057	860	-0.41	63.9
04	0	95	0.44	606	287	-0.71	82.3
05	0	97	0.15	770	373	-0.85	63.9
06	1	97	0.45	732	353	-0.66	89.1
07	0	100	0.27	1653	1255	-0.39	71.6
08	0	100	0.48	1282	647	-0.41	69.8
09	0	100	0.55	2288	2962	-0.01	51.3
10	0	100	0.22	2290	1211	-0.17	54.8
11	0	100	0.39	977	2892	-0.24	69.4
12	0	100	0.29	1014	2180	-0.39	77.9
13	0	100	0.52	1221	875	-0.45	67.8
14	0	100	0.19	1736	898	-0.33	68.6
15	1	100	0.59	2636	1410	-0.25	69.5
16	0	100	0.25	1417	721	-0.43	79.2
17	0	100	0.09	1249	1120	-0.39	77.3
18	1	100	0.53	4266	2373	0.09	39.4
19	0	100	0.60	2201	2245	-0.08	51.8
20	1	96	0.37	631	302	-0.91	75.6
21	0	100	0.66	2775	2904	-0.09	70.0
22	0	100	0.16	1239	1273	-0.40	80.6
23	1	100	0.33	2587	1382	-0.13	54.1
24	0	100	0.28	1136	2467	-0.31	77.7
25	0	100	0.58	1997	1045	-0.27	62.4
26	0	100	0.86	1572	1152	-0.42	71.1
27	0	100	0.69	2133	6204	-0.13	53.3
28	1	100	0.84	2810	3479	0.06	49.4
29	1	100	0.69	5116	6650	0.32	46.9
30	1	100	0.511	2856	3182	0.06	50.2
31	0	100	0.501	1910	3724	-0.05	44.6
32	0	100	0.345	1890	3652	-0.03	44.7
33	0	100	0.407	2708	2136	0.03	58.1
34	0	100	0.422	1346	2675	-0.28	64.6
35	0	100	0.231	2230	1860	-0.32	54.4
36	0	93	0.088	633	665	-0.48	77.6
37	1	100	0.715	1477	2156	-0.34	78.3
38	0	84	-0.754	598	457	-0.62	81.4
39	0	100	0.781	1751	906	-0.32	71.2
40	1	100	0.413	792	384	-0.67	71.8
41	1	94	0.286	617	293	-0.89	84.9
42	0	100	0.361	921	1111	-0.61	89.6

43	0	100	0.08	1449	738	-0.45	68.1
44	0	92	-0.353	967	703	-0.61	68.4
45	0	100	-0.048	785	934	-0.65	94.1
46	0	97	-0.106	786	936	-0.55	88.1
47	1	94	-0.037	621	882	-0.69	62.6
48	0	100	0.423	2049	3617	0.06	53.7
49	3	91	0.182	549	316	1.07	5.6
50	0	70	-0.277	107	44	-1.89	96.8
51	0	100	0.355	1751	3684	-0.06	55.9
52	0	90	-0.056	544	629	-0.55	100.6
53	0	100	0.505	1598	3754	-0.07	64.1
54	0	100	0.56	1732	1601	-0.23	62.8
55	1	97	0.322	872	426	-0.61	77.6
56	0	84	-0.174	371	383	-0.73	82.1
57	0	100	0.321	1325	671	-0.67	80.3
58	1	100	0.789	2443	6359	-0.19	54.5
59	1	100	-0.024	2040	1069	-0.28	61.9
60	1	100	0.535	1855	965	-0.23	57.2
61	0	78	-0.055	129	197	-0.46	67.3
62	2	100	1.071	2211	1856	-0.04	56.3
63	0	100	0.72	1406	2083	-0.39	64.1
64	0	100	-0.176	1492	1258	-0.31	60.0
65	0	100	0.341	1190	1053	-0.34	87.8
66	0	100	0.613	2448	1302	-0.18	59.8
67	1	100	0.353	782	379	-0.75	72.8
68	1	89	0.328	398	183	-0.92	84.9
69	0	100	-0.386	1532	784	-0.39	70.1
70	0	100	-0.204	1626	1499	-0.14	70.7
71	0	100	-0.296	1715	1554	-0.14	74.6
72	1	100	0.598	2550	1361	-0.19	51.1
73	0	100	0.307	683	748	-0.43	73.4
74	0	100	0.432	780	2004	-0.26	75.6
75	0	100	0.9	2952	1594	-0.29	51.7
76	0	100	0.104	1045	925	-0.54	73.5
77	1	100	0.392	837	408	-0.65	69.8
78	0	100	0.704	936	821	-0.53	71.74

%HOA: percentage of human oral absorption; logKhsa: binding to human serum albumin; pCaco-2: intestinal cells; pMDCK: renal cells; plogBB: blood-brain barrier permeation; and PSA: Van der Waals surface area.

All molecules presented favorable Stars values results, except for molecule 49. Despite this molecule presented stars = 3, which should indicate low reliability, other parameters evaluated in this study were within the stipulated limits for the calculations. Only two molecules showed results indicating low oral absorption in terms of %HOA: 50 and 61. All other molecules showed results indicating for high oral absorption. With regard to aggregation to plasma albumin protein, all results indicate less aggregation to albumin than rimonabant. Most molecules showed indicative results for high cell permeability in pCaco and pMDCK. However, molecules 04, 05, 06, 20, 38, 40, 41, 55 and 67 showed medium permeability in pMDCK; and molecules 50, 56, 61 and 68 showed medium results for both.

Most of them were within the indicative parameters for blood-brain barrier permeability, with results > -1. Only molecule 50 showed results indicating non-permeation (plogBB = -1.89). The others, although presenting a prediction to permeate such barrier, have more satisfactory results than rimonabant (<1.5), indicating less affinity.

Regarding PSA, molecules that may be administered orally acting peripherally (PSA > 70) were: 01, 02, 04, 06, 07, 12, 16, 17, 20-22, 24, 26, 36-42, 45, 46, 50, 52, 55-57, 65, 67-71, 73, 74, 76 e 78. Only the zinc molecule 49 had PSA lower than that of rimonabant.

Therefore, with regard to pharmacokinetic properties, ZINC molecules that fitted within the desired criteria for parameters, and also that presented predictions indicating higher chances of being administered orally and with high

chances of acting peripherally (PSA > 70 and logP < 4) and act peripherally are: 01, 02, 04, 06, 07, 12, 16, 17, 20, 22, 36-38, 40-42, 45, 46, 52, 55-57, 67-71, 73 e 78.

Analysis of toxicological properties

Results obtained in the DEREK software were analyzed considering the following toxicological endpoints: mutagenicity, carcinogenicity, peroximal proliferation, hepatotoxicity, genotoxicity, neurotoxicity and reproductive effects. This software generates its output results using different confidence levels for each corresponding endpoint: CERTAIN (active), PROBLABLE (probable), PLAUSIBLE / EQUIVOCAL (evidence is not strong / toxicity is not certain), DOUBTED (inactive but doubtful due to lack of experimental evidence) and IMPROBABLE / INATIVE (unlikely).[33]

Rimonabant presented alerts for carcinogenicity (EQUIVOCAL) and HERG channel inhibition (PLAUSIBLE). When analyzing phytocannabinoids no alerts were fired in relation to their genotoxicity, neurotoxicity or reproductive effects endpoints. Molecule 24 presented human toxicity alerts regarding nephrotoxicity (equivocal) and hepatotoxicity (equivocal), referring to the styrene or derivative toxicophore. Molecule 32 showed alert for hepatotoxicity (plausible for the p-alkylphenol or derivative toxicophore). Such plausible and equivocal results do not indicate strong evidence of these toxicities and can only be confirmed by experimental evaluation.[31,33]

Given the results obtained for the toxicological properties of phytocannabinoids, molecules 29 and 35 presented the best safety profile (no toxicity alerts), but did not present satisfactory results for activity and ADME predictions. Thus, considering the predictions of biological activity and physicochemical properties, molecules that allow an additional *in silico* evaluation to elucidate their mode of interaction in relation to our study objective, phytocannabinoids 01, 06, 07, 15 and 37 were considered, which present results for the prediction of toxicity even safer than those of Rimonabant.

The 78 molecules that were selected from the ZINC database were also evaluated in the DEREK software. All alerts have been fired as PLAUSIBLE, and their evidence of uncertainty can be confirmed or ruled out by experimental evaluation.[31,33] The results are summarized below:

- **Human hepatotoxicity**: PLAUSIBLE for molecules 01, 09, 12, 14, 15, 19, 21, 22, 24, 27, 41-43, 45, 46 and 52, having as a toxicophore the benzimidazole or derivative radical, except for molecule 01, which its toxicophore was the furan radical;
- **Human carcinogenicity:** PLAUSIBLE alert for molecule 50, referring to the aromatic group amine or amide;
- **Human *in vivo* mutagenicity**: PLAUSIBLE for molecule 25, referring to the quinoline group;
- **Cyanidine-type effect alert:** for molecule 05, referring to the nitrile group, considered PLAUSIBLE;
- **Chromosome Damage Alert:** PLAUSIBLE for molecule 78 concerning the toxicophore group indole or benzotriazole;

The best profile ZINC molecules, considering the predictions of biological activity (anti-obesity activity potential >0.4) and physicochemical, pharmacokinetic and toxicological properties (safer than rimonabant), which were selected for *in silico* evaluation to better comprehend their interaction modes towards our target of interest are molecules 06, 17, 20, 38, 67, 69 and 70.

Molecular Docking Analysis

Molecular docking analysis was based on the results of Shao and collaborators[34] which conducted CB1 receptor molecular anchoring experiments in inactive conformation with PDB ID: 5U09. Validation by redocking [35] has been performed with a RMSD of 1.269 Å, as shown in Figure 4, when superimposing the originally complexed ligand taranabant from protein 5U09 (in green), and the best pose obtained from molecular docking (in blue). This result shows greater reliability when compared to the RMSD of Loo and collaborators [36], which was 2.74 Å for the best pose of antagonist AM115424 on the same protein.

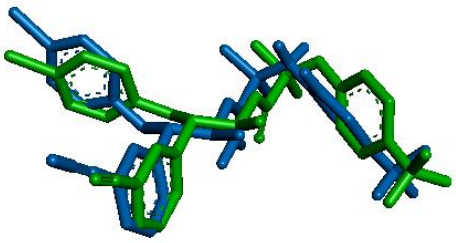

Figure 4. Docking Validation showing original ligand taranabant from complex 5U09 in green, and the best pose obtained from molecular docking in blue.

The rCB1 structure has seven transmembrane domains (TM) connected through three extracellular loops (ECL1-3) and three intracellular loops (ICL1-3). The N-terminal domain has a V-shaped loop formed by residues 99-111 that acts as a lid and is, therefore, responsible for favoring or restricting access of a binder to the pouch from the extracellular side.[37]

In rCB1 structure (PDB ID: 5U09), the complexed antagonist molecule was taranabant, and the main interactions that occur between these molecules and rCB1, favorable to antagonism, are related to the following amino acids: Phe102, Met103, Asp104, Ile105, Phe108, Ile119, Ser123, Ile169, Phe170, Phe174, Leu193, Val196, Phe268, Trp279, Trp356, Leu359, Met363, Phe379, Ala380, Met384, Cys386 e Leu387.[34]

Filling the orthosteric pouch at the opening of TM1 and TM7 acts by blocking the entry of endocannabinoids, contributing to this blocking the amino acids Ile119 (TM1), Phe381 and Met384 (TM7). Interactions with with amino acid residues of these two helices should favor the inactive conformation of receptor. Leu387 belongs to the membrane access channel and favors the closing of entrance channel, along with the amino acids mentioned above. TM1 is formed by residues Asn112 to Ser144, while TM7 is formed by residues Asn372 to Arg400. Arg214 and Asp338 favor canonical ion blockade. Lys192, Phe200 and Tyr275 indirectly contribute to conformational equilibrium, even without interacting with the antagonist. THC agonist binding is favored by Phe174, Leu193 and Ser383.[34]

Met103, Ile105, Phe108, Ile119, Phe170, Phe268, Trp279, Trp356, Phe379 and Leu387 are characterized by involvement in taranabant and rimonabant binding affinity, but are part of the binding pool of agonists and antagonists.[34] ECL2 (Trp255-Ile271) has 4 residues (Phe268-Ile271) next to the TM5 which when projected into the binding bag mediated interactions that decrease agonist binding. ECL3 is associated with decreased flexibility of this loop region.[37]

The interactions that occur with the residues Phe170 and Phe174, from TM2, favor the inclination in relation to TM1 (Arg150-Val179), while the interaction with Lys192 (from TM3) decreases the affinity of agonists and stabilizes the conformation of ECL1, from the domain N-terminal and extracellular part of TM2 and TM3, [37] in addition to moving the receptor to its inactive state. [23]

Murineddu and collaborators,[38] when docking antagonist AM6538 into the rCB1 structure (PDB ID: 5TGZ), obtained a new hydrogen bond, now with Ser383, also important in antagonist binding. This docking study showed relevant amino acids from the active site within 10 Å: Phe102, Met103, Ile105, Ile119, Ser123, Ile169, Phe170, Phe174, His178, Leu193, Val196, Thr197, Phe268, Leu276, Val279, Val356, Leu359, Met363, Ala380, Ser383, Met384, C386 e Leu387.

Finally, proceeding as described in materials and methods, we present our docking results, revealing potential interactions of Rimonabant (Fig 5) and the five selected phytocannabinoids that showed best physicochemical, pharmacokinetic, toxicological profile, among those with Pa >0.4 in the PASS prediction, which were: 01 (Fig. 6), 06 (Fig. 7), 07 (Fig. 8), 15 (Fig. 9) and 37 (Fig. 10). Although they did not present a pharmacokinetic profile favorable to peripheral action, knowing their way of binding to rCB1 allows obtaining additional parameters for analyzing the interaction of the virtual screening molecules on the ZINC server.

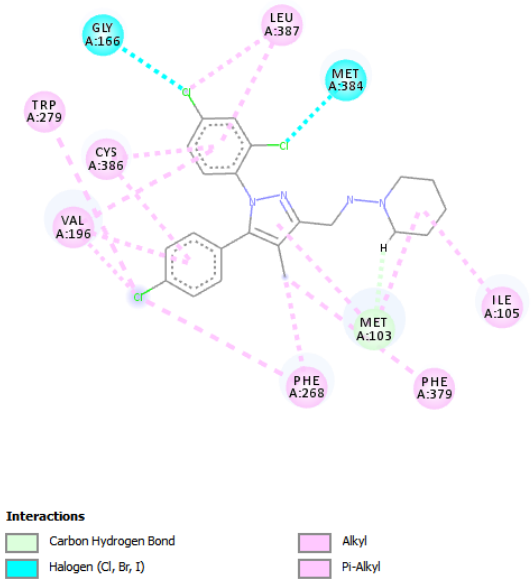

Figure 5: Molecular docking of Rimonabant.

The rimonabant presented GoldScore of 86.20, performing a total of 12 interactions with the active site, with 10 amino acid residues belonging to the N-terminal domains (Met103 and Ile105), TM2 (Gly166), TM3 (Val196), ECL2 (Phe268), TM5 (Trp279) and TM7 (Phe379, Met384, Cys386 and Leu387).

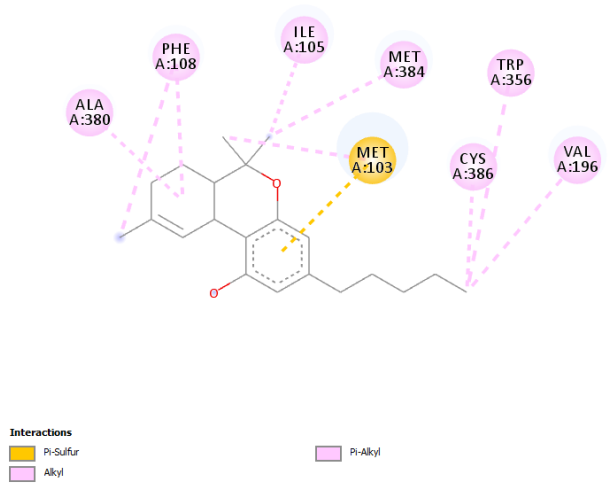

Figure 6. Molecular docking of phytocannabinoid 01 (Δ^9-THC).
Cannabinoid 01 had a GoldScore of 73.44 and was able to perform ten interactions with the binding site within the 5.2 Å radius, mostly hydrophobic (pink strokes). Their interactions occurred in the N-terminal domain (Met103, Ile105 and Phe108), TM3 (Val196), TM6 (Trp356) and TM7 (Ala380, Met384 and Cys386).

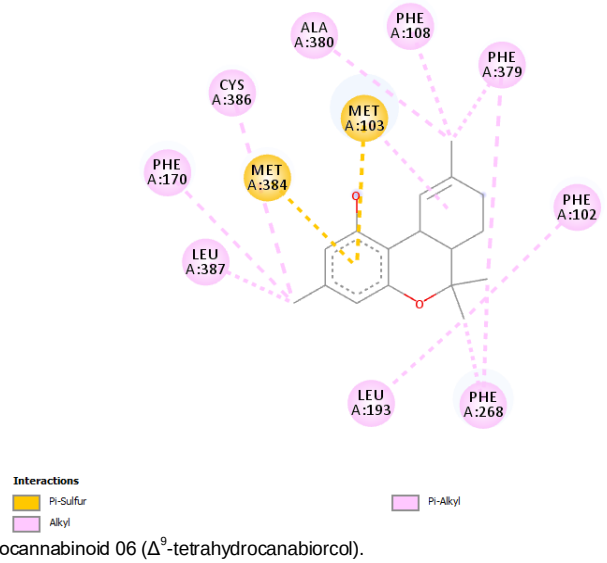

Figure 7. Molecular docking of phytocannabinoid 06 (Δ^9-tetrahydrocanabiorcol).
Cannabinoid 06 had a GoldScore of 55.79, the smallest of the six molecules presented, and was able to perform fourteen interactions with the binding site within a 5.4Å radius. Their interactions occurred in the N-terminal (Phe102, Met103 and Phe108), ECL2 (Phe268), TM2 (Phe170), and TM7 (Phe379, Ala380, Met384, Cys386 and Leu387) domains.

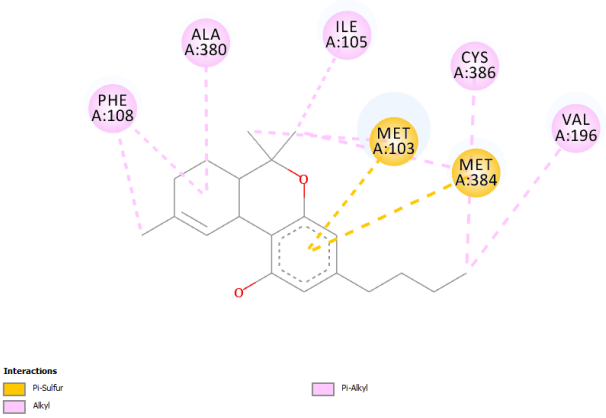

Figure 8. Molecular docking of phytocannabinoid 07 (Δ^9-tetrahydrocanabiorcol-C_4).
Cannabinoid 07 had a GoldScore of 69.11 and was able to perform ten interactions with the binding site within the 5.6Å radius. Their interactions occurred in the N-terminal domain (Phe102, Ile105 and Phe108), TM3 (Val196) and TM7 (Ala380, Met384 and Cys386).

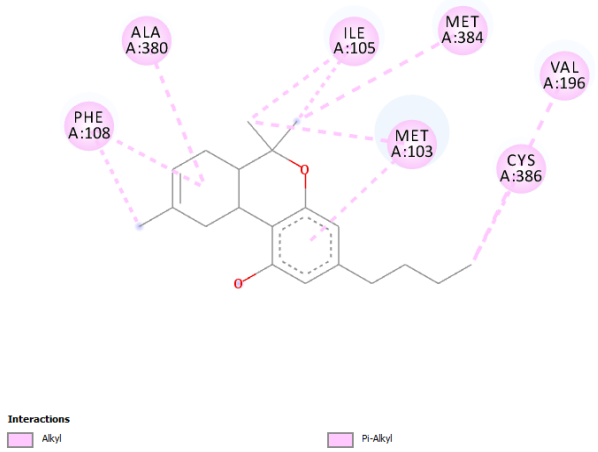

Figure 9. Molecular docking of phytocannabinoid 15 (Δ^8-THC).
Cannabinoid 15 had a GoldScore of 69.63 and performed ten interactions with the binding site within a radius of 4.9Å (the smallest interaction radius). Interactions occurred at N-terminal (Met103, Ile105 and Phe108), TM3 (Val196) and TM7 (Ala380, Met384 and Cys386).

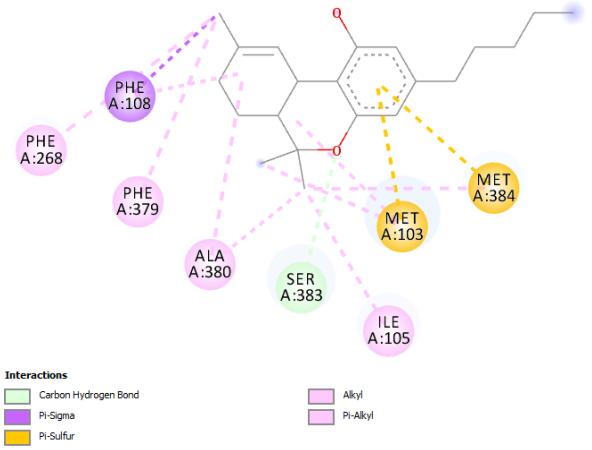

Figure 10. Molecular docking of phytocannabinoid 37 (cis-Δ^9-THC).
Cannabinoid 37 presented GoldScore of 75.46, the largest of the phytocannabinoids evaluated, and performed thirteen interactions with the binding site, within a 5Å radius. Interactions occurred at N-terminal (Met103, Ile105 and Phe108), ECL2 (Phe268) and TM7 (Phe379, Ala380, Ser383 and Met384).

The rCB1 orthosteric pocket shows hydrophobic characteristics, since this receptor is activated by lipids,[34] which explains the fact that the vast majority of occurring interactions are hydrophobic. All phytocannabinoids interacted with the N-terminal domain (mostly hydrophobic bonds), which is related to restriction of membrane access by ligands

from the extracellular side.[37] All had a radius of interaction with the active site below 10 Å, none showed interaction with Lys192, but molecule 37 (Fig. 10) made an important hydrogen bond with Ser383.[38]

The molecule with the smallest radius of interaction with active site residues was 15 (Fig. 9), which hinders for an agonist to enter by reducing the access channel, although it has interacted only with seven amino acid residues of three transmembrane domains (including Met384). Rimonabant (Fig. 5) performed hydrogen bonding between Met103 and the HD region of the rimonabant. Its GoldScore was not surpassed by phytocannabinoids, the closest result being that of molecule 37. The molecule that presented the greatest interaction with the transmembrane domains was molecule 06 (Fig. 7), displaying fourteen interactions with eleven amino acid residues (including Phe170, Met384 and Leu387). However, it had the lowest GoldScore of the ranking (55.79).

Molecule 01 (Fig. 6) is known for its CNS psychotropic action on the CB1 receptor as an agonist. It presented a high GoldScore (73.44) and interacted with eight amino acid residues from four domains (including Met384) without showing hydrogen bonds. Molecule 07 (Fig 8) interacted with only seven amino acid residues from three transmembrane domains (including Met384), also without presenting hydrogen interactions in the antagonist interaction.

Molecule 37 (Fig. 10) interacted with eleven (four domains) and eight (three domains) amino acid residues, respectively, showing hydrogen bonds with Ser383, and other interactions to residues Phe268 and Met384.

Regarding the docking of ZINC molecules, the following results reveal the anchoring of molecules 06 (Fig. 11), 17 (Fig. 12), 20 (Fig. 13), 38 (Fig. 14), 67 (Fig. 15), 69 (Fig. 16) and 70 (Fig. 17). These were the ones with better physicochemical, pharmacokinetic and toxicological profile among those that had, in PASS prediction, rCB1 antagonist activity and anti-obesity activity, with Pa > 0.4. Docking results showing specific interactions occurring between these ZINC molecules and the active site are shown in figure are shown below.

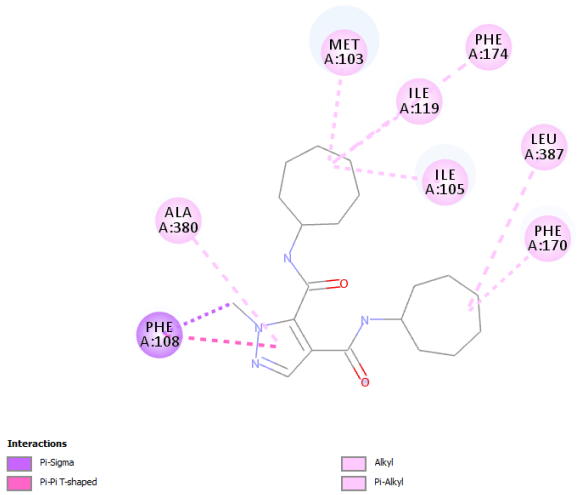

Figure 11. Molecular docking of **ZINC 06** (ZINC20616264).
The ZINC 06 molecule had a GoldScore of 76.67 and performed eight interactions with the binding site within a radius of 5.3Å. Interactions occurred at N-terminal (Met103, Ile105 and Phe108), TM1 (Ile119), TM2 (Phe170 and Phe174) and TM7 (Ala380 and Leu387).

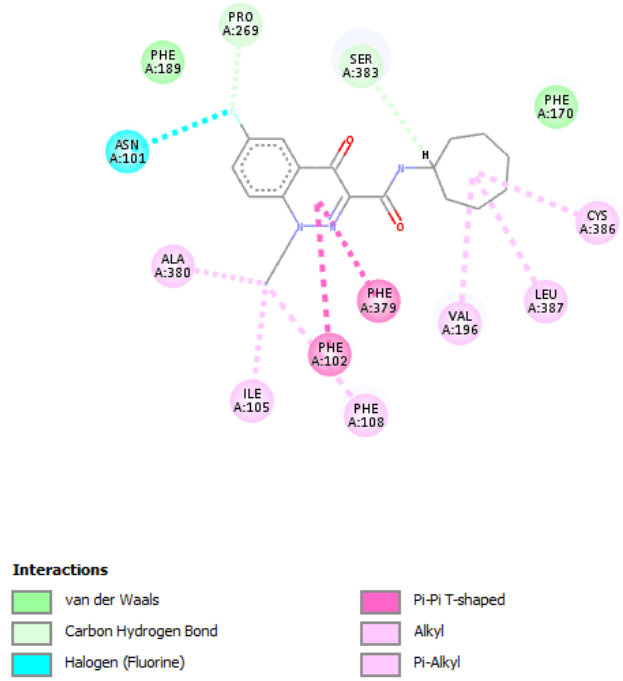

Figure 12. Molecular docking of **ZINC 17** (ZINC40791167).
The ZINC 17 molecule had a GoldScore of 78.19 and performed twelve interactions with the binding site within a radius of 5.9Å. Interactions occurred at N-terminal (Asn101, Phe102, Ile105 and Phe108), TM2 (Phe170), TM3 (Val196), ECL2 (Pro269) and TM7 (Phe379, Ala380, Ser383, Cys386 and Leu387).

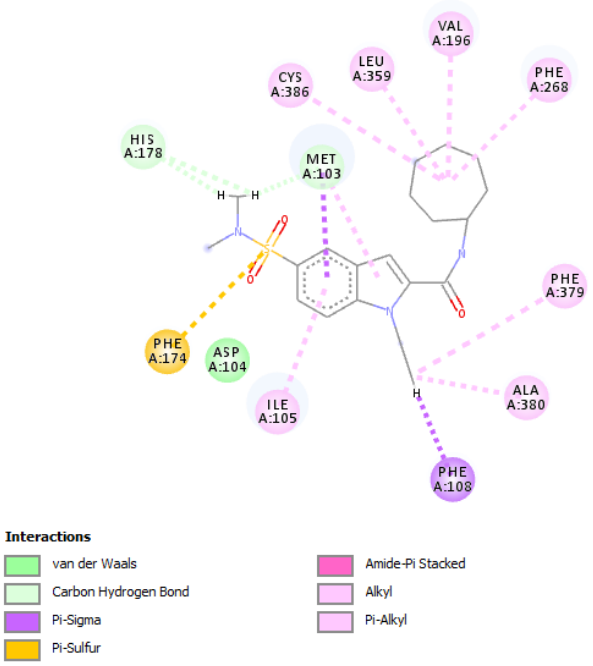

Figure 13. Molecular docking of **ZINC 20** (ZINC46031287).
The ZINC 20 molecule had a GoldScore of 82.97 and performed fourteen interactions with the binding site within a radius of 5.9Å. Interactions occurred at N-terminal (Met103, Asp104, Ile105 and Phe108), TM2 (Phe174 and His178), TM3 (Val196), ECL2 (Phe268), TM6 (Leu359) and TM7 (Phe379 and Ala380).

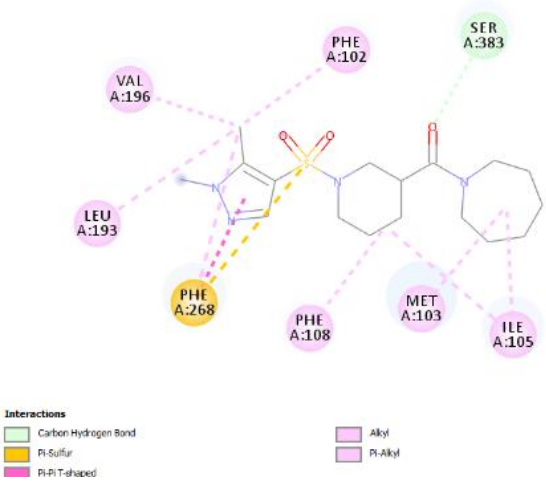

Figure 14. Molecular docking of **ZINC 38** (ZINC2732822).
The ZINC 38 molecule had a GoldScore of 74.79 and performed eleven interactions with the binding site within a 5.4Å radius. Interactions occurred at N-terminal (Phe102, Met103, Ile105 and Phe108), TM3 (Val196), ECL2 (Phe268) and TM7 (Ser383).

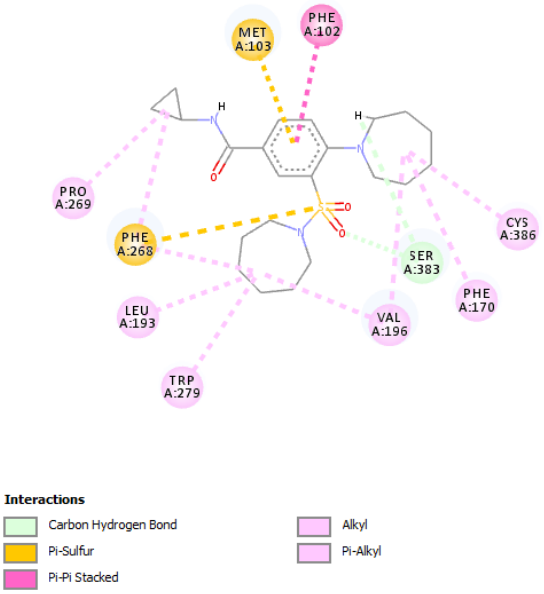

Figure 15. Molecular docking of **ZINC 67** (ZINC33053400).
The ZINC 67 molecule had a GoldScore of 79.83 and performed thirteen interactions with the binding site within a radius of 5.67Å. Interactions occurred at N-terminal (Phe102 and Met103), TM2 (Phe170), TM3 (Leu193 and Val196), ECL2 (Phe268), TM5 (Trp279) and TM7 (Ser383 and Cys386).

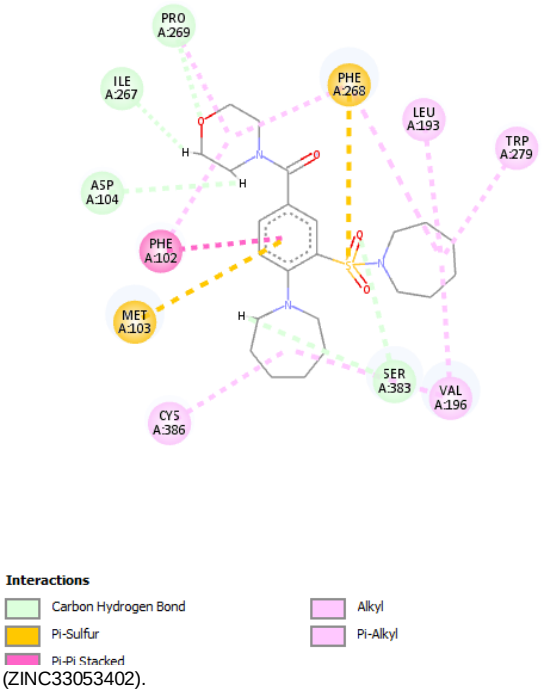

Figure 16. Molecular docking of **ZINC 69** (ZINC33053402).
The ZINC 69 molecule had a GoldScore of 80.28 and performed eighteen interactions with the binding site within a radius of 5.44Å. Interactions occurred at N-terminal (Phe102, Met103 and Asp104), TM3 (Leu193 and Val196), TM5 (Trp279) ECL2 (Ile267, Phe268 and Pro269) and TM7 (Ser383 and Cys386).

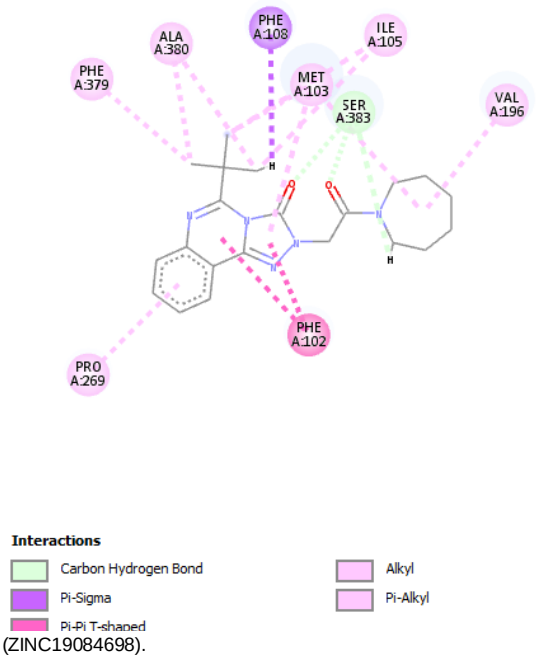

Figure 17. Molecular docking of **ZINC 70** (ZINC19084698).
The ZINC 70 molecule had a GoldScore of 87.29 and performed eleven interactions with the binding site within a radius of 5.7Å. Interactions occurred at N-terminal (Phe102, Met103 and Phe108), TM3 (Val196), ECL2 (Pro269) and TM7 (Ala380 and Ser383).

The ZINC molecule 06 (Fig. 11) did not show hydrogen bond with Ser383, but showed a high value of GoldScore, which was 76.67, higher than phytocannabinoid 37 (75.46), however less than that of rimonabant. It interacted with eight amino acids from four domains, in a radius of 5.3 Å, having as key residues Ile119, Phe170, Phe174 and Leu387, which favor the blockade of the anandamide endocannabinoid entrance by closing the entrance channel by tilting towards TM1.

The Zinc 17 molecule interacted with five transmebranal domains, including N-terminal, ECL2 and TM7, its GoldScore was close to 80, performing interactions with more amino acid residues from the active site (12) than rimonabant (10), performing interactions of hydrogen between Ser383 and hydrogen donor region, and between Pro269 hydrogen acceptor region. The zinc 20 molecule had a GoldScore of 82.97, performing 14 interactions with the active site in six transmembrane domains. It performed Hydrogen bonds between Met103 and His178 and the molecule's hydrogen donor region.

The ZINC molecule 38 (Fig. 13) also interacted with eight active site amino acid residues, showing a greater number of favorable interactions, totaling eleven, in four domains within a radius of 5.3 Å. Its GoldScore of 74.79 was slightly lower than that of phytocannabinoid 37, and it presented two key interactions with Phe268 and a hydrogen bond with Ser383, which reduces endocannabinoid agonist binding and favors greater interaction strength and stability.

The zinc 67 molecule had a higher GoldScore than phytocannabinoid 37, but no higher than rimonabant. It performed 13 interactions with the active site in six transmembrane domains, with two hydrogen bonds between Ser383 and the hydrogen donor and acceptor region.

The zinc 69 molecule had the highest number of interactions with the active site (18) in five transmembrane domains, with GoldScore greater than 80. It performed hydrogen bonds between Ser383 and the hydrogen acceptor region, and between Pro269 and region hydrogen donor. The zinc 70 molecule was the one that had the best result in docking. Its GoldScore of 87.29, surpassing that of rimonabant (86.20), performing eleven interactions with four transmembrane domains, including three hydrogen bonds with Ser383 and hydrogen acceptor regions.

Evaluating the results, it can be seen that the phytocannabinoid molecules did not exceed the docking parameters of the rimonabant molecule. Now the zinc molecules present better quality docking, surpassing rimonabant in GoldScore (zinc molecule 70), and in quantity of interactions with the active site (zinc molecules 17, 20, 67 and 69), where all interacted with the domains transmembrane-related antagonist activity in rCB1. The two best molecules were zinc 69 and 70 that had a prediction of anti-obesity activity > 0.5 and with GoldScores values 80.29 and 87.29, respectively, the latter being superior to the reference ligand rimonabant, showing that these are molecules potential for future studies of anti-obesity activity.

Conclusions

Molecular modeling studies performed in this work allowed us to disclose that the selected phytocannabinoids evaluated here, have shown to be potential rCB1 antagonists, according to their predicted biological activities by the PASS server. Moreover, docking results showed a broad possibility of stablishing key interactions between these molecules and the receptor, considering GoldScores values greater than the original ligand taranabant from the crystallographic structure. It is worth to note that the phytocannabinoid that would most likely present a strong tendency to act as a rCB1 antagonist, with interest in anti-obesity activity, is molecule 37, since it presented a relevant hydrogen bond with Ser383 that is essential for antagonists activity. However, all have prediction of action in the CNS, profile that is related to the triggering of adverse reactions inherent to the pharmacological target studied.

In fact, when comparing to another virtual screening campaigns previously found in the literature, our virtual screening performance showed promising results, because it was able to achieve potential molecules with positive predictions for rCB1 antagonism and also indicated their potential to possess anti-obesity activity, with Pa > 0.4. Their corresponding docking results were also significant, since it was observed similar interactions to the reference and GoldScores values greater than 80.00, with the highest result for the zinc 70 molecule surpassing rimonabant, and this may suggest binding affinities as intense as those observed for phytocannabinoids. To sum up, the best profile screened ZINC molecules to act as rCB1 antagonist in peripheral antiobesity activity were 69 e 70 (for presenting key binding for the blockade of anandamide endocannabinoid agonist and the high GoldScores). In addition, these molecules have a possible factor favorable to the safety of the use of a peripheral level cannabinoid antagonist, due to its pharmacokinetic profile, which may overcome the barriers of adverse effects inherent in this pharmacological class.

Experimental Section

Design and optimization of molecules

The design of the chemical structure of the 104 phytocannabinoid molecules presented by Pertwee[16] was performed in the **ChemSketch v2007 2.1** program and their structures were geometrically optimized in the **HyperChem v8.0** program, using the semi-empirical method RM1 (*Recife Model 1*), in order to get structures with minimal conformational energy.

Prediction of biological activity and pharmacophore derivation

Prediction of biological activity was performed on the **PASS** server[39] (*Predicition of Activity Spectra for Substances*) (http://www.way2drug.com/PASSOnline/) to identify those molecules that have CB1 receptor antagonist activity. From the 32 best results, then, the pharmacophoric pattern was derived in the **PharmaGist** server[18] (http://bioinfo3d.cs.tau.ac.il/PharmaGist/) to obtain the biological activity regions of the cluster.[21]

Virtual screening

Performed on the **ZINCPharmer** web server (http://zincpharmer.csb.pitt.edu/),[24] which identifies molecules by similarity of hydrophobic, aromatic, hydrogen donor and acceptor regions, positive and negative ions. Molecules selected from the ZINCpharmer

web server have the same pharmacophoric regions previously predicted for phytocannabinoids. Compounds that combine with a well-defined pharmacophorus will serve as potential leaders for the possible discovery of rCB1 acting drugs through molecular modeling.

The filter used for screening was: subset zinc purchasable; Max Hits per conf: 1; Max Hits per Mol: 1; Max total hits: 1000; e Max RMSD: 1,5; 0 ≤ Molecular Weight ≤ 500, 0 ≤ Rotatable Bonds ≤ 8.

Physicochemical properties

Physicochemical properties were identified on the **PubChem** server (http://www.ncbi.nlm.nih.gov/pccompound) for phytocannabinoids and on the **ZINC** server (http://zinc.docking.org/) for the screened molecules on the ZINCpharmer server. These data allow the assessment, by Lipinski's Rule of Five[25], of the oral absorption of each molecule through its molecular weight, logP, and number of hydrogen donors and acceptors.

Prediction of pharmacokinetic and toxicological properties of phytocannabinoids and Zinc molecules

To predict the pharmacokinetic properties of absorption, distribution, metabolism and excretion (ADME), the **QikProp** software[29] was used to calculate the parameters: stars, percent human oral absorption (% HOA), cellular permeability in Caco2 (pCaco-2) and MDCK (pMDCK), human serum albumin binding (plogKhsa), Van de Waals surface area (PSA), and blood-brain barrier permeability (pLogBB). Toxicological properties were determined by nephrotoxicity, hepatotoxicity, carcinogenicity and mutagenicity predictions in the **DEREK NEXUS 2.1** software,[33] using as a prediction filter for humans.

Molecular Docking Simulation

Docking analysis was performed using **GOLD 5.7.1** (*Genetic Optimization for Ligand Docking*) software to predict the binding of molecules with better physicochemical, pharmacokinetic and toxicological profile to deal with rCB1. The crystallographic structure of rCB1 complexed with an antagonist (taranabant) was obtained from the Protein Data Bank (PDB) server under the PDB ID: 5U09, with a resolution of 2.6 Å. Validation of binding at the binding site, that is, reproduction of the ligand conformation occurs by redocking calculating Root Mean-Square-Deviation (RMSD), which must have been less than 2 Å. The highest score anchors are those whose chemical structures have the most favorable binding free energy to bind to the binding site.[40]

Protein preparation involved the addition of hydrogens, the extraction of water molecules, as well as the deletion of all ligands present in the structure, with ligand A09 being taranabant. Ligand A09 was selected in the binding site definition step for the program to detect the binding cavity, restricting the selection of atoms to solvent and keeping the surface accessible. The phytocannabinoids and screening molecules evaluated (Zinc molecules) were pre-optimized in HyperChem under the RM1 semi-empirical method and inserted into the following binding site coordinates: x = 21.66, y = 3.21 and z = -9.06.

Conflict of interest

The authors declare no conflict of interest.

Keywords: Molecular Docking. Structure-activity relationship. Natural cannabinoids. rCB1. Virtual Screening.

References:

[1] N. Srivastava, R. Lakhan, B. Mittal, *Indian Journal of Experimental Biology* **2007**, *45*, 929–936.
[2] M. S. Ibsen, M. Connor, M. Glass, *Cannabis and Cannabinoid Research* **2017**, *2*, 48–60.
[3] WHO, "Obesidade e excesso de peso," **2017**.
[4] M. N. Hawkins, T. L. Horvath, *Journal of Clinical Investigation* **2017**, *127*, 3918–3920.
[5] C. P. Yonaha, Análise Comportamental Clínica No Tratamento Da Obesidade, Instituto Brasiliense de Análise do Comportamento, **2016**.
[6] S. Y. Romero-Zerbo, F. J. Bermúdez-Silva, *Drug Testing and Analysis* **2014**, *6*, 52–58.
[7] F. Akbas, C. Gasteyger, A. Sjödin, A. Astrup, T. M. Larsen, *Obesity Reviews* **2009**, *10*, 58–67.
[8] G. G. Szabo, N. Lenkey, N. Holderith, T. Andrasi, Z. Nusser, N. Hajos, *Journal of Neuroscience* **2014**, *34*, 7958–7963.
[9] A. I. Fraguas- Sánchez, A. M. Fernández-Carballido, A. I. Torres-Suárez, *Anales de la Real Academia Nacional de Farmacia* **2014**, *80*, 555–577.
[10] A. L. Marcia, P. N. Edgar, F. R. Pola, C. M. Pia, *Revista Medica de Chile* **2017**, *145*, 360–367.
[11] M. A. ElSohly, *Marijuana and the Cannabinoids*, Humana Press, Totowa, New Jersey, **2007**.
[12] W. Milano, M. F. Tecce, A. Capasso, *Diseases and Disorders* **2017**, *1*, 1–6.
[13] A. F. de Godoy-Matos, E. P. Guedes, L. L. de Souza, C. M. Valério, *Arquivos brasileiros de endocrinologia e metabologia* **2006**, *50*, 390–399.
[14] S. Engeli, A.-C. Lehmann, J. Kaminski, V. Haas, J. Janke, A. A. Zoerner, F. C. Luft, D. Tsikas, J. Jordan, *Obesity* **2014**, *22*, E70–E76.
[15] G. Burdyga, S. Lal, A. Varro, R. Dimaline, D. G. Thompson, G. J. Dockray, *The Journal of neuroscience : the official journal of the Society for Neuroscience* **2004**, *24*, 2708–15.
[16] R. G. Pertwee, *Handbook of Cannabis*, Oxford University Press, United Kingdom, **2014**.
[17] R. M. de Paulo, B. S. de Abreu, *Revista de Divulgação Científica Sena Aires* **2015**, *4*, 62–69.
[18] M. A. Elsohly, M. M. Radwan, W. Gul, S. Chandra, A. Galal, *Phytocannabinoids*, Springer International Publishing, Cham, **2017**.
[19] World Health Organisation, *WHO* **2014**.
[20] F. Colon-Gonzalez, G. W. Kim, J. E. Lin, M. A. Valentino, S. A. Waldman, *Molecular Aspects of Medicine* **2013**, *34*, 71–83.
[21] D. Schneidman-Duhovny, O. Dror, Y. Inbar, R. Nussinov, H. J. Wolfson, *Nucleic acids research* **2008**, *36*, W223-8.
[22] M. K. Sharma, P. R. Murumkar, G. Kuang, Y. Tang, M. R. Yadav, *RSC Advances* **2016**, *6*, 1466–1483.
[23] H. Wang, R. A. Duffy, G. C. Boykow, S. Chackalamannil, V. S. Madison, *Journal of Medicinal Chemistry* **2008**, *51*, 2439–2446.

[24] D. R. Koes, C. J. Camacho, *Nucleic acids research* **2012**, *40*, W409-14.
[25] C. A. Lipinski, F. Lombardo, B. W. Dominy, P. J. Feeney, *Advanced Drug Delivery Reviews* **1997**, *23*, 3–25.
[26] M. K. Sharma, J. Machhi, P. Murumkar, M. R. Yadav, *Scientific Reports* **2018**, *8*, 1650.
[27] Ajay, G. W. Bemis, M. A. Murcko, *Journal of Medicinal Chemistry* **1999**, *42*, 4942–4951.
[28] G. N. Lee, K. R. Kim, S. H. Ahn, M. A. Bae, N. S. Kang, *Bioorganic and Medicinal Chemistry Letters* **2010**, *20*, 5130–5132.
[29] Schrödinger, **2012**.
[30] J. M. Luco, *Journal of Chemical Information and Computer Sciences* **1999**, *39*, 396–404.
[31] M. C. Sharma, *Medicinal Chemistry Research* **2014**, *23*, 2287–2311.
[32] J. Kelder, P. D. J. Grootenhuis, D. M. Bayada, L. P. C. Delbressine, J. P. Ploemen, *Pharmaceutical Research* **1999**, *16*, 1514–1519.
[33] F. Ntie-Kang, C. V. Simoben, B. Karaman, V. F. Ngwa, P. N. Judson, W. Sippl, L. M. Mbaze, *Drug design, development and therapy* **2016**, *10*, 2137–54.
[34] Z. Shao, J. Yin, K. Chapman, M. Grzemska, L. Clark, J. Wang, D. M. Rosenbaum, *Nature* **2016**, *540*, 602–606.
[35] J. C. Cole, C. W. Murray, J. W. M. Nissink, R. D. Taylor, R. Taylor, *Proteins: Structure, Function and Genetics* **2005**, *60*, 325–332.
[36] J. S. E. Loo, A. L. Emtage, L. Murali, S. S. Lee, A. L. W. Kueh, S. P. H. Alexander, *RSC Advances* **2019**, *9*, 15949–15956.
[37] T. Hua, K. Vemuri, M. Pu, L. Qu, G. W. Han, Y. Wu, S. Zhao, W. Shui, S. Li, A. Korde, et al., *Z.J.L. Cell* **2016**, *167*, 750–762.
[38] G. Murineddu, F. Deligia, G. Ragusa, L. García-Toscano, M. Gómez-Cañas, B. Asproni, V. Satta, E. Cichero, R. Pazos, P. Fossa, et al., *Bioorganic and Medicinal Chemistry* **2018**, *26*, 295–307.
[39] D. A. Filimonov, A. A. Lagunin, T. A. Gloriozova, A. V. Rudik, D. S. Druzhilovskii, P. V. Pogodin, V. V. Poroikov, *Chemistry of Heterocyclic Compounds* **2014**, *50*, 444–457.
[40] S. Roy, B. K. Narang, M. K. Gupta, V. Abbot, V. Singh, R. K. Rawal, *Drug Research* **2018**, *68*, 395–402.

Entry for the Table of Contents

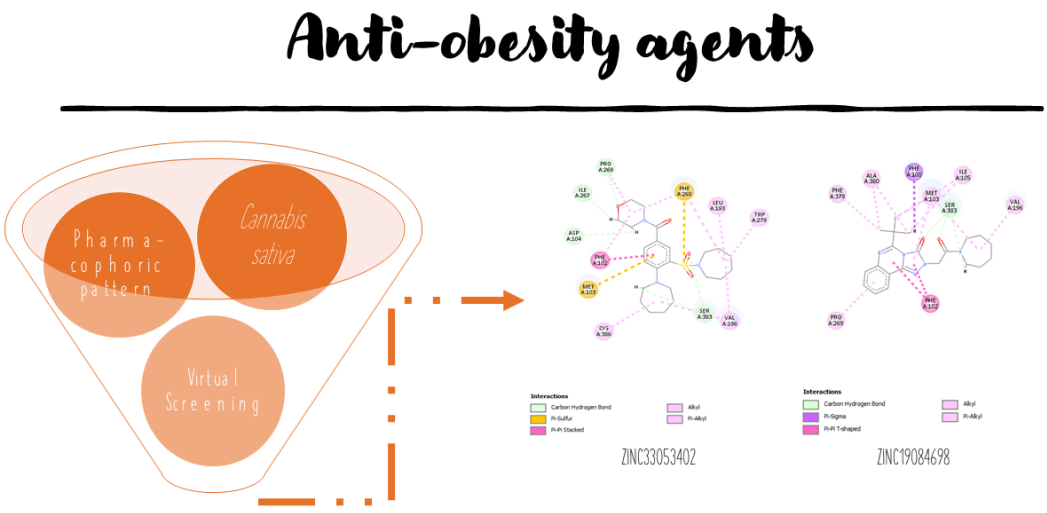

Virtual screening of new anti-obesity agents. The construction of a pharmacophoric pattern for screening anti-obesity agents based on *C. sativa* phytocannabinoids aims at proposing new agents that may prove to be safer and more effective. Based on the rCB1 antagonism, two ZINC molecules gained prominence: ZINC33053402 and ZINC19084698.

4 CONSIDERAÇÕES FINAIS E PERSPECTIVAS.

A busca por novos fármacos é uma corrida diária que visa principalmente a segurança do paciente. Realizar uma triagem virtual baseada em canabinoides de *C. sativa* buscou investigar mais um dos diversos potenciais farmacêuticos que essa planta proporciona. Desta vez, a ação antiobesidade é avaliada devido ao potencial destes metabólitos sobre o receptor canabinoide 1, já utilizado anteriormente para a ação dos fármacos Rimonabanto e Taranabanto. O resultado da busca revelou um padrão farmacofórico de cinco pontos que, ao ser submetido às análises propostas apresentou resultados promissores para duas moléculas, com potencial para atuação antiobesidade e antagonismo rCB1, na base de dados ZINC de substâncias possíves de serem adquiridas (ZINC33053402 e ZINC19084698). Os resultados de uma triagem virtual permitiram selecionar racionalmente moléculas que possam vir a ser mais seguras e efetivas para a ação antiobesidade, condição metabólica que tem sua incidência aumentada na população mundial. Como perspectiva futura pretende-se, então, dar prosseguimento aos estudos das duas moléculas selecionadas para avaliar *in vivo* sua segurança e o seu real potencial antiobesidade.

REFERÊNCIAS

AKBAS, F. et al. A critical review of the cannabinoid receptor as a drug target for obesity management. **Obesity Reviews**, v. 10, n. 1, p. 58–67, 2009.

BURDYGA, G. Expression of Cannabinoid CB1 Receptors by Vagal Afferent Neurons Is Inhibited by Cholecystokinin. **Journal of Neuroscience**, v. 24, n. 11, p. 2708–2715, 2004.

COLON-GONZALEZ, F. et al. Obesity pharmacotherapy: What is next? **Molecular Aspects of Medicine**, v. 34, n. 1, p. 71–83, 2013.

DESPRÉS, J.-P. **Abdominal Obesity and the Endocannabinoid System**. [s.l.] CRC Press, 2008.

ELSOHLY, M. A. **Marijuana and the Cannabinoids**. Totowa, New Jersey: Humana Press, 2007.

ELSOHLY, M. A. et al. **Phytocannabinoids**. Cham: Springer International Publishing, 2017. v. 103

ENGELI, S. et al. Influence of dietary fat intake on the endocannabinoid system in lean and obese subjects. **Obesity**, v. 22, n. 5, p. E70–E76, 2014.

FONSECA, B. M. et al. O Sistema Endocanabinóide - uma prespetiva terapêitica. Acta Farmacêutica Portuguesa, v. 2, n. 2, p. 97–104, 2013.

FRAGUAS-SÁNCHEZ, A. I.; FERNÁNDEZ-CARBALLIDO, A. M.; TORRES-SUÁREZ, A. I. Cannabinoids: A promissing tool for the development of novel therapies. **Anales de la Real Academia Nacional de Farmacia**, v. 80, n. 3, p. 555– 577, 2014.

FRAHER, D. et al. Lipid Abundance in Zebrafish Embryos Is Regulated by Complementary Actions of the Endocannabinoid System and Retinoic Acid Pathway. **Endocrinology**, v. 156, n. 10, p. 3596–3609, 1 out. 2015.

GODOY-MATOS, A. F. DE et al. The endocannabinoid system: a new paradigm in the metabolic syndrome treatment. **Arquivos brasileiros de endocrinologia e metabologia**, v. 50, n. 2, p. 390–399, 2006.

HAWKINS, M. N.; HORVATH, T. L. Cannabis in fat: High hopes to treat obesity. **Journal of Clinical Investigation**, v. 127, n. 11, p. 3918–3920, 2017.

HODAVANCE, S. Y. et al. G Protein–coupled Receptor Biased Agonism. Journal of Cardiovascular Pharmacology, v. 67, n. 3, p. 193–202, 1 mar. 2016.

IBSEN, M. S.; CONNOR, M.; GLASS, M. Cannabinoid CB 1 and CB 2 Receptor Signaling and Bias. **Cannabis and Cannabinoid Research**, v. 2, n. 1, p. 48–60, 2017.

LEWIS, M. M. et al. Chemical Profiling of Medical Cannabis Extracts. ACS Omega, v. 2, n. 9, p. 6091–6103, 2017.

MARCIA, A. L. et al. Potencial uso terapéutico de cannabis. **Revista Medica de Chile**, v. 145, n. 3, p. 360–367, 2017.

MILANO, W.; F. TECCE, M.; CAPASSO, A. The role of endocannabinoids in the control of eating disorders. **Diseases and Disorders**, v. 1, n. 1, p. 1–6, 2017.

PAULO, R. M. DE; ABREU, B. S. DE. Cannabis No Gerenciamento De Patologias-Revisão De Literatura Cannabis in the Management ofPathologies- Literature. **Revista de Divulgação Científica Sena Aires**, v. 4, n. 2, p. 62–69, 2015.

PERTWEE, R. G. **Handbook of Cannabis**. 1st. ed. United Kingdom: Oxford University Press, 2014.

ROMERO-ZERBO, S. Y.; BERMÚDEZ-SILVA, F. J. Cannabinoids, eating behaviour, and energy homeostasis. **Drug Testing and Analysis**, v. 6, n. 1–2, p. 52–58, 2014.

SRIVASTAVA, N.; LAKHAN, R.; MITTAL, B. Pathophysiology and genetics of obesity. **Indian Journal of Experimental Biology**, v. 45, n. 11, p. 929–936, 2007.

SZABO, G. G. et al. Presynaptic Calcium Channel Inhibition Underlies CB1 Cannabinoid Receptor-Mediated Suppression of GABA Release. **Journal of Neuroscience**, v. 34, n. 23, p. 7958–7963, 2014.

YONAHA, C. P. **Análise Comportamental Clínica no Tratamento da Obesidade**. [s.l.] Instituto Brasiliense de Análise do Comportamento, 2016.

VIGITEL BRASIL. **Hábitos dos brasileiros impactam no crescimento da obesidade e aumenta prevalência de diabetes e hipertensão**. Disponível em: <http://portalarquivos.saude.gov.br/images/pdf/2017/abril/17/Vigitel.pdf>. Acesso em: 1 maio. 2018.

WHO. **Obesidade e excesso de peso**. Disponível em: <http://www.who.int/en/news-room/fact-sheets/detail/obesity-and-overweight>. Acesso em: 29 apr. 2018.

ZLEBNIK, N. E.; CHEER, J. F. Beyond the CB1 Receptor: Is Cannabidiol the Answer for Disorders of Motivation? Annual Review of Neuroscience, v. 39, n. 1, p. 1–17, 2016.

ANEXOS

Anexo 1– Normas de publicação da revista ChemMedChem – Chemistry Enabling Drug Discovery (Wiley Online Library)

Title

Author(s),[b] and Corresponding Author(s)*[a]

Dedication ((optional))

[a] Title(s), Initial(s), Surname(s) of Author(s) including Corresponding Author(s)
Department
Institution
Address 1
E-mail:
[b] Title(s), Initial(s), Surname(s) of Author(s)
Department
Institution
Address 2

Supporting information for this article is given via a link at the end of the document.((Please delete this text if not appropriate))

Abstract: Insert abstract text here. ((Abstracts should be 800-1000 characters in length excluding spaces. Please ensure your abstract is written so that it can be read in isolation (i.e., in an abstracting service such as PubMed), with all abbreviations defined.))

Introduction

Main Text Paragraph.

Results and Discussion

Main Text Paragraph.

((Insert Scheme here. **Note:** Please do **not** combine scheme and caption in a textbox or frame.))

Scheme 1. Scheme Caption.

Main Text Paragraph.

((Insert Figure here. **Note:** Please do **not** combine figure and caption in a textbox or frame.))

Figure 1. Figure Caption.

Main Text Paragraph.

Table 1. Table Caption. ((**Note:** Please do **not** include the table in a textbox or frame))

Head 1[a]	Head 2	Head 3[b]	Head 4[c]	Head 5
Column 1	Column 2	Column 3	Column 4	Column 5
Column 1	Column 2	Column 3	Column 4	Column 5

[a] Table Footnote. [b] …

Conclusion

Main Text Paragraph.

Experimental Section

Experimental Details.

Acknowledgements ((optional))

Acknowledgements Text.

Keywords: keyword 1 • keyword 2 • keyword 3 • keyword 4 • keyword 5

[1] ((Reference 1, **Example for Journals**:)) a) A. Author, B. Coauthor, *ChemSusChem***2008**, *1*, 1-10; b) A. Author, B. Coauthor, *Angew. Chem.***2006**, *118*, 1-5; *Angew. Chem. Int. Ed.***2006**, *45*, 1-5.

[2] ((Reference 2: **Example for Books**:)) J. W. Grate, G. C. Frye in *Sensors Update*, *Vol. 2* (Eds.: H. Baltes, W. Göpel, J. Hesse), Wiley-VCH, Weinheim, **1996**, pp. 10-20.

[3] …

Entry for the Table of Contents

Insert graphic for Table of Contents here. ((Please ensure your graphic is in **one** of following formats))

((max. width: 5.5 cm; max. height: 5.0 cm))

Please delete this box prior to submission

((max. width: 11.5 cm; max. height: 2.5 cm))

Please delete this box prior to submission

Instructions on how to include a double-column width figure, scheme or table:

- Place the insertion point where you want to change the number of columns.
- On the *Layout* tab, in the *Page Setup* group, click **Breaks** and select **Continuous**.
- Ensure the insertion point is in the new section and on the *Layout* tab, in the *Page Setup* group, click **Columns** and select **One**.
- A figure, scheme or table inserted into this section will now span two columns.
- Finally, add another section break after the figure, scheme or table and change it back to two columns.

Please delete this box prior to submission

Insert text for Table of Contents here. ((The Table of Contents text should give readers a short preview of the main theme of the research and results included in the paper to attract their attention into reading the paper in full. The Table of Contents text **should be different from the abstract** and should be no more than 450 characters including spaces.))

Institute and/or researcher Twitter usernames: ((optional))